

General Disclaimer

One or more of the Following Statements may affect this Document

- This document has been reproduced from the best copy furnished by the organizational source. It is being released in the interest of making available as much information as possible.
- This document may contain data, which exceeds the sheet parameters. It was furnished in this condition by the organizational source and is the best copy available.
- This document may contain tone-on-tone or color graphs, charts and/or pictures, which have been reproduced in black and white.
- This document is paginated as submitted by the original source.
- Portions of this document are not fully legible due to the historical nature of some of the material. However, it is the best reproduction available from the original submission.

NASA CR-144656

15 APRIL 1975

EXPERIMENT DEFINITION PHASE
SHUTTLE LABORATORY

LDRL-10.6 EXPERIMENT

Third Quarterly Report

N75-29164

Unclas
33361

CSCI 22E G3/18

(NASA-CF-144656) EXPERIMENT DEFINITION
PHASE SHUTTLE LAECRATCRY LDRL-10.6
EXPERIMENT Quarterly Report, 26 Dec. 1974 -
26 Mar. 1975 (Hughes Aircraft Co.) 124 p HC
\$5.25 CSCI 22E G3/18

NASA Contract NAS 5-20018



HUGHES

HUGHES AIRCRAFT COMPANY
SPACE AND COMMUNICATIONS GROUP

CONTENTS

	<u>Page</u>
1. INTRODUCTION AND SUMMARY	
1.1 Introduction	1
1.2 Program Objectives	2
1.3 Historical Background	4
1.4 Scope	6
1.5 Program Schedule	8
2. LINK PERFORMANCE SUMMARY	
2.1 Summary	11
2.2 Link Geometry	12
2.3 Orbit Imposed Experiment Link Parameters	14
2.4 Acquisition Procedure and Parameters	16
2.5 Communication Performance Requirements	18
2.6 Link Design Control Tables	20
2.7 Constants Used in Design Control Table Calculations	22
2.8 Transmitter and Receiver Weight and Power Tabulations	24
3. ACQUISITION AND TRACKING	
3.1 Summary	27
3.2 Requirements	28
3.2.1 Shuttle to Ground Link	28
3.2.2 Shuttle to Molniya	30
3.2.3 Image Motion Compensator	32
3.2.4 Gimbal Servo	34
3.2.5 Fine Track and Lead Angle Corrector	36
3.3 System Block Diagram	38
4. OPTOMECHANICAL SUBSYSTEM DESIGN	
4.1 Summary	41
4.2 Gimbal/Structure Layout Review	42
4.2.1 General Operational Concept and Program Goals	42
4.2.2 System Parameters for Upgraded Flyable Experiment	44
4.2.3 Transmitter Coordinate System	46
4.2.4 Overall Optomechanical Subsystem Packaging	48
4.2.5 Mechanical Design Considerations for Testing in a Gravitational Field and Overall Mechanical Requirements	50
4.2.6 General Arrangement of Gimbals and Optics	52
4.2.7 Beryllium Telescope Box Structure	54
4.2.8 Bearing Analysis	
4.2.9 End View of Gimbal Package	58
4.2.10 Instrument Gearing Arrangement	60
4.2.11 Base Compartment	62
4.2.12 Conceptual Base Compartment Content and Arrangement	64

PRECEDING PAGE BLANK NOT FILMED

4.2.12	Conceptual Base Compartment Content and Arrangement	64
4.2.13	IMC Device Concepts	66
4.2.14	Two Large Folding Mirrors	68
4.2.15	Relay Mirror Adjustment Device	70
4.2.16	Focusing Element Adjustment	72
4.2.17	Procured Items	74
4.3	Optics Design Layout Review	76
4.3.1	Optics Design Summary	76
4.3.2	Selected Optical Design	78
4.3.3	Optical Design Constraints/Specifications	80
4.3.4	Beam Matching and Energy Transfer	82
4.3.5	Optical Schematic Overview	84
4.3.6	Optical Layout	86
4.3.7	7X Gregorian Beam Expander	88
4.3.8	Optical Characteristics of 7X Gregorian Beam Expander	90
4.3.9	6X Gregorian Pre-Expander	92
4.3.10	Optical Characteristics of 6X Gregorian Pre-Expander	94
4.3.11	Optical Layout Showing Locations of Elements 1 Through 13	96
4.3.12	Preliminary Beryllium Component Drawings	98
4.3.12.1	Element 1: Flat Pointing Mirror	100
4.3.12.2	Element 2: Flat Folding Mirror	102
4.3.12.3	Element 3: Primary Mirror	104
4.3.12.4	Element 4: Secondary Mirror	106
4.3.12.5	Element 5: Small Folding Mirror	108
4.3.12.6	Elements 6 and 7: Two Flat IMC Mirrors	110
4.3.12.7	Elements 8 and 9: Two Flat Folding Mirrors	112
4.3.12.8	Elements 10 Through 13: Pre-Expander Assembly Mirrors	114
4.3.13	Material	116
5.	OPTOMECHANICAL SUBSYSTEM AND 10 MICROMETER RECEIVER MEASUREMENTS	119

1. Introduction and Summary

1.1 INTRODUCTION

This third quarterly report for the Experiment Definition Phase of the Shuttle Laboratory LDRL 10.6 Experiment (Contract NAS 5-20018) covers the period from 26 December 1974 to 26 March 1975. During this quarter, the design and layout of the transmitter optomechanical subsystem brassboard model was essentially completed. This effort culminated in a formal Design Layout Review on 27 March 1975. The material presented at that review forms the basis for this quarterly report and documents the LDRL-10.6 program activities during the past quarter as well as overall program status. All charts presented at the review are shown either as tables or figures, with accompanying descriptive text as appropriate.

Third quarter program activities included:

- 1) Update of the LDRL Design Control Table to detail the transmitter optical chain losses and incorporate the change to a reflective beam pre-expander
- 2) Continued examination of the link establishment sequence, including its dependence upon spacecraft stability
- 3) Design of the transmitter pointing and tracking control system
- 4) Finalization of the transmitter brassboard optical and mechanical design

1. Introduction and Summary

1.2 PROGRAM OBJECTIVES

The LDRL 10.6 program is directed toward applying optical communications to NASA's wideband data transmission requirements through the 1980's. To accomplish this objective, development contracts have been let by NASA for the elements of a 10.6 μm laser data relay link (LDRL 10.6) design. In its deployed form, the LDRL will consist of a transmitter on one or more low earth orbit satellites with an elliptical orbit satellite receiver. Other links of eventual interest include direct downlinks to ground from both these terminals, synchronous to synchronous satellite two-way links, and synchronous satellite to ground links.

OBJECTIVE AND DEVELOPMENT CONTRACTS

OBJECTIVE

Investigate one approach to satisfy NASA's wideband data requirements for late 1970's and 1980's.

DEVELOPMENT CONTRACTS

Laser transmitter on low earth orbit satellite

Elliptical orbit receiver with doppler tracking capability

Transceiver for synchronous to synchronous satellite applications

50150-1T

1. Introduction and Summary

1.3 HISTORICAL BACKGROUND

The current contract (NAS 5-20018) is directed toward definition of an LDRL experiment for the Shuttle Laboratory to verify the feasibility of an operational LDRL system. In addition, the present contract is being extended to include the development of the 10.6 μm transmitter optomechanical subsystem brassboard model. The latter task complements and continues previous LDRL 10.6 efforts. Contract NAS 5-20623, originally intended for the transmitter package, was redirected toward CO₂ laser tube development. Contract NAS 5-21859 has developed the 10.6 μm receiver optomechanical subsystem brassboard.

PERTINENT NASA LASER CONTRACTS AWARDED TO HUGHES

NAS 5-20018, Experiment Definition for Shuttle Sortie Laboratory LDRL 10.6 Experiment
(being extended to include the optomechanical subsystem of the 10 μ m transmitter)
NAS 5-20623, 10 μ m Transmitter
(Modified to emphasize CO₂ laser tube development)
NAS 5-21859, Optomechanical Subsystem of 10 μ m Receiver

50150-2T

1. Introduction and Summary

1.4 PROGRAM SCOPE

The present program is divided into two phases. The first phase consists of 1) definition and planning of the communication experiment, 2) determination of the ensuing system requirements, and 3) design of the requisite 10.6 μm shuttle transmitter optomechanical subsystem. At the end of the first phase the effort will stop pending the completion of tests on associated NASA laser communication equipment, the optomechanical subsystem with its receiver. During the second phase, appropriate test results will be combined with the phase 1 work and published in the final report.

A third phase is planned. It is the fabrication, assembly, and checkout of the transmitter optomechanical subsystem brassboard model designed under this study. The fabricated brassboard optomechanical subsystem is intended to be updated later to a functional engineering model transmitter, which could possibly be used on the Shuttle Spacelab.

PROGRAM SCOPE

- Experiment definition of Shuttle Sortie Laboratory LDRL-10.6 experiment
- Develop the brassboard* optomechanical subsystem for the Shuttle LDRL-10.6 transmitter terminal (pending follow-on effort authorization)

50150-3T

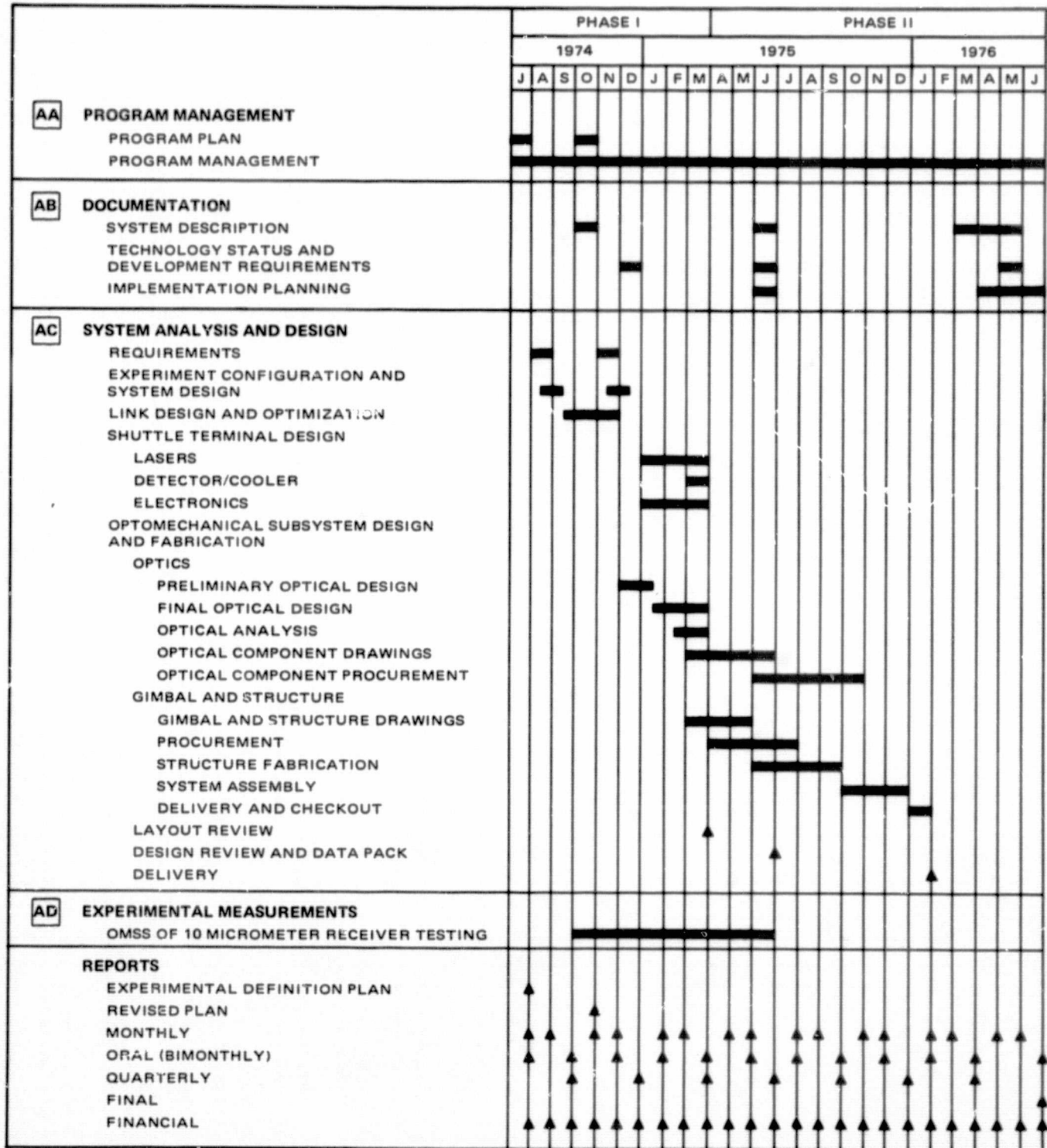
*Consists of the basic structure, gimbal mechanism, and telescope. The brassboard model will be able to be updated eventually to a fully functional engineering model transmitter possessing communication capability and a servo control subsystem.

1. Introduction and Summary

1.5 PROGRAM SCHEDULE

At the conclusion of the third quarter the program is on schedule. Analysis and design of the optomechanical subsystem has been concluded as have all prior indicated tasks. Essentially all optomechanical subsystem component drawings have been completed.

The final test phases of the optomechanical receiver have been delayed 2 months due to the delayed procurement of the waveguide local oscillator. This is a no-cost delay. Previous testing has demonstrated the ability of the optical subsystem to acquire and track an optical source.



PROGRAM SCHEDULE

2. Link Performance Summary

2.1 SUMMARY

The LDRL 10.6 link analysis program has been revised to reflect the final transmitter brassboard optical system configuration. The program generated Design Control Table now includes a correspondingly more detailed description of transmitter optical chain losses. In the following topics, the LDRL operational environment is briefly described. Design Control Tables are presented for the most critical communication link for both the experimental and the deployed LDRL systems. The corresponding transmitter and receiver package weight breakdowns are also discussed.

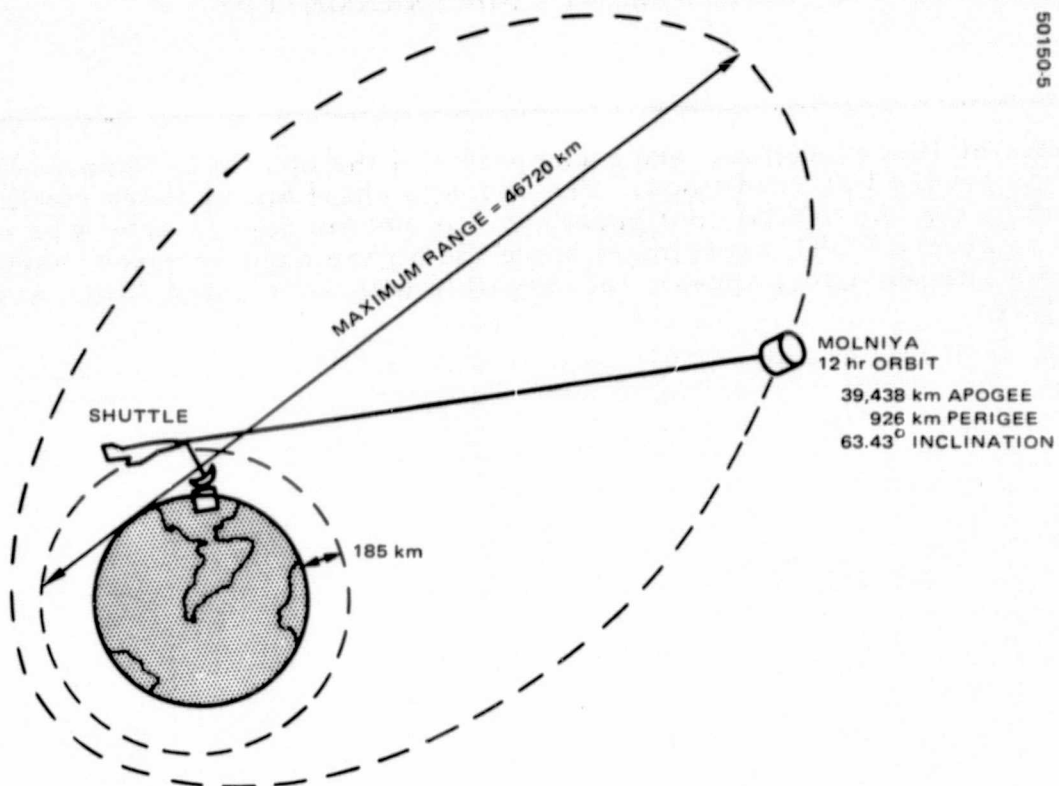
PRECEDING PAGE BLANK NOT FILMED

2. Link Performance Summary

2.2 LINK GEOMETRY

The LDRL 10.6 Experiment is designed for two generic communication links:

1) Shuttle to ground station and 2) Shuttle to Molniya orbit satellite. It has been established that the full range of orbit imposed parameters encountered to candidate LDRL links is enveloped by these two situations. Each link utilizes the LDRL 10.6 transmitter on the Shuttle Spacelab. Shuttle orbits are assumed to be circular with altitudes ranging from 185 to 500 km. The Molniya orbit is a minimal apsidal rotation orbit inclined at 63.043° with an apogee of 38,438 km and a perigee of 926 km. The indicated maximum communication range occurs for a 185 km Shuttle orbit coplaner with the Molniya.



LINK GEOMETRY

2. Link Performance Summary

2.3 ORBIT IMPOSED EXPERIMENT LINK PARAMETERS

The extreme link conditions are a composite of the Shuttle to Molniya link and the Shuttle to ground link conditions. The opposite chart shows these conditions as imposed by the two orbital configurations. A 500 km Shuttle orbit was chosen for the Shuttle to ground LDRL experiment since the higher angular rates associated with the lower altitude orbits appear incompatible with anticipated LDRL acquisition capabilities.

ORBIT IMPOSED PARAMETERS

Parameter	Extreme Value	Orbital Condition
Range	46,720 km	Shuttle to Molniya
Doppler	942 MHz	Shuttle to Molniya
Point ahead angle	86 μ rad	Shuttle to ground
Angular rate	48 deg/min	Shuttle to ground (500 km orbit)

50150-6T

2. Link Performance Summary

2.4 ACQUISITION PROCEDURE AND PARAMETERS

Deployed Case. The deployed case is an ultimate operational system. It is compatible with the experiment but has some improved parameters.

The higher orbit relay satellite, in contact with the ground control station, can serve a number of low earth orbiting satellites. On ground command, the relay satellite initiates the link establishment procedure by illuminating the corresponding low earth orbiting satellite with a 4.0 watt CO₂ beacon of 0.13° beamwidth. The low earth orbiting satellite scans its acquisition (uncertainty) angle of $\pm 0.5^\circ$ with its instantaneous field of view of 55.94 μ rad and detects the relay satellite with a probability 0.99 in 5.41 seconds. The low earth orbiting satellite acquisition angle $\pm 0.5^\circ$ is based on the assumption that it will have this pointing accuracy capability. Then the transmitter of the low earth orbiting satellite is turned on, and the relay satellite acquires it in 1.08 seconds by scanning the acquisition angle of $\pm 0.1^\circ$ with its instantaneous field of view of 36.9 μ rad. The tracking and communication phase then starts on command from the relay satellite.

Experiment Case. In the experiment case, the Shuttle initiates the link establishment procedure by illuminating the Molniya satellite with a 1.0 watt CO₂ beacon of 0.13° beamwidth. The experimental package in the Molniya orbit has a 16.51 cm aperture and scans its acquisition angle of $\pm 0.13^\circ$ with its instantaneous field of view of 66.1 μ rad. It detects the Shuttle in 1.40 seconds. The Molniya orbit satellite then turns on its 1 watt CO₂ transmitter. Its 66.1 μ rad transmitter beamwidth is coaxial with the received beacon and therefore illuminates the Shuttle. The Shuttle beacon receiver now scans the shuttle acquisition angle of $\pm 0.5^\circ$ (actually reduced by the Shuttle Spacelab Instrument Pointing System to $\pm 0.06^\circ$) and acquires the Molniya in 5.41 seconds, with a probability 0.99. The Shuttle broadbeam beacon is then switched to its communication transmitter beamwidth of 55.94 μ rad, and the tracking and communication phase starts.

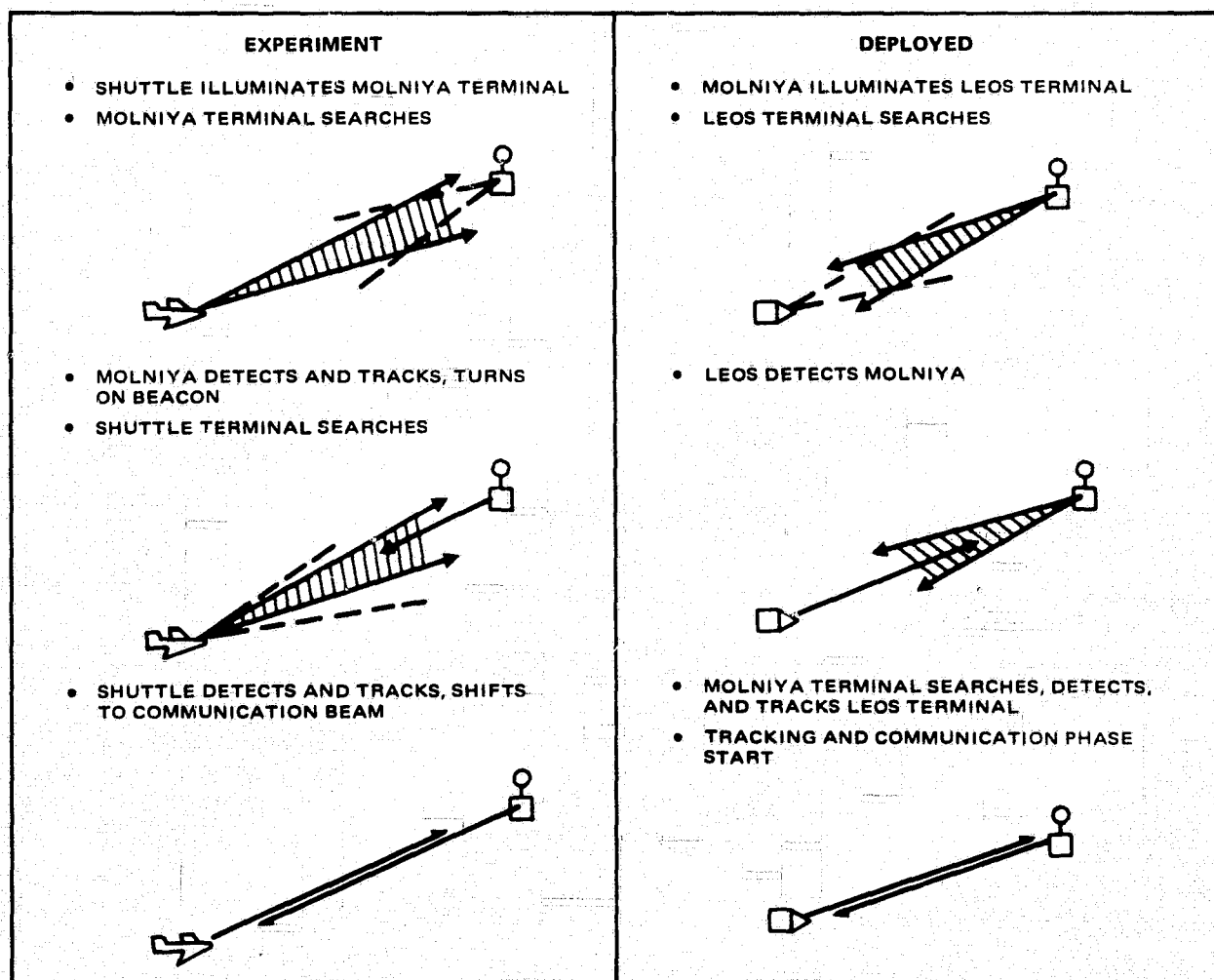
Allowance for point ahead compensation hardware has been made. The uncompensated point ahead loss depends upon point ahead angle, but could be as large as 6 dB. Point ahead compensation should be made, but a detailed control design has not yet been incorporated.

ACQUISITION PARAMETERS

Parameter	Low Earth Orbiting Satellite (Transmitter)		Molniya (Receiver)	
	Shuttle Experimental	Deployed	Experimental	Deployed
Aperture, cm	18.0	18.0	16.51	29.57
Obscuration (diameter)	0.417	0.417	0.200	0.200
Instantaneous field of view, μ rad	55.94	55.94	66.13	36.92
Communication transmitter, power, W	1.0	1.0	1.0*	-
NEP, $W \cdot Hz^{-1}$	5.35×10^{-20}	5.35×10^{-20}	5.35×10^{-20}	5.35×10^{-20}
Beacon power, W	1.0	-	-	4.0
Beacon beamwidth, deg	0.12	-	-	0.13
Acq. uncertainty angle, deg	± 0.5	± 0.5	± 0.13	± 0.1
Probability of acquisition**	0.99	0.99	0.99	0.99
Mean acquisition time, sec	5.41	5.41	1.40	1.08

*Presently is planned as a transceiver.

**False alarm probability 10^{-3} .



LINK ESTABLISHMENT PROCEDURE

50150-8T

50150-7

2. Link Performance Summary

2.5 COMMUNICATION PERFORMANCE REQUIREMENTS

The deployed LDRL performance requirement is stipulated to be a data rate capability of 400 Mbps with a 10^{-6} bit error probability, P_e . In an experimental test using the existing optomechanical subsystem the data rate would be reduced to 124.67 Mbps corresponding to the smaller OMSS experimental receiver aperture, 16.51 cm, while retaining the same P_e .

The system IF bandwidth, B_{IF} , requirement is a function of the link data rate, R_b . The low pass bandwidth, B_o , corresponding to B_{IF} is $B_o = B_{IF}/2$. For a given detection method, the detector performance degradation from the ideal matched filter case due to thermal noise and intersymbol interference depends on the ratio B_o/R_b . The relationship between B_o/R_b and detector performance degradation has been examined for a number of detection methods. One readily implemented detection scheme for binary digital data uses the "band limit and sample" detector. For this situation, the detector performance degradation may be minimized by the optimal choice of B_o/R_b . The detector performance degradation may be characterized by the increase in P_e (for constant bit energy/spectral noise density, E_b/N_o) or alternatively, by the increase in E_b/N_o required to maintain a constant P_e . For the LDRL 10.6 requirement of $P_e = 10^{-6}$, the detector performance degradation is minimized for $B_o/R_b = 0.88$. The corresponding required IF bandwidth for the LDRL 400 x 10^6 bps data rate is then

$$\begin{aligned} B_{IF} &= 2 B_o \\ &= 2 \times 0.88 \times R_b \\ &= 704 \times 10^6 \text{ Hz} \end{aligned}$$

The corresponding required $(S/N)_{IF}$ to detect with specified P_e depends on the detection method used. For the chosen band limit and sample scheme, required $(S/N)_{IF}$ is determined by B_o/R_b . For $P_e = 10^{-6}$ and the corresponding optimum value of $B_o/R_b = 0.88$, the E_b/N_o required is approximately 17.6 (12.3 dB). The $(S/N)_{IF}$ is then determined.

$$\begin{aligned} (S/N)_{IF} &= \left(\frac{E_b}{N_o} \right) / \left(\frac{B_{IF}}{R_b} \right) \\ &= 9.75 \text{ or } 9.9 \text{ dB} \end{aligned}$$

An additional 6 dB margin is included to accommodate design uncertainties. The resultant $(S/N)_{IF} = 15.9$ dB has been used as a basis for the LDRL system performance calculations.

COMMUNICATION PERFORMANCE REQUIREMENTS

Parameter	Value
Data rate, R_b	400 MBps
Bit error rate, P_e	10^{-6}
Required bit energy/noise spectral density, E_b/N_0	12.3 dB
Optimal output bandwidth/data rate, B_o/R_b	0.88
Required IF bandwidth, $B_{IF} = 2 B_o = 1.76 R_b$	704 MHz
Required IF signal to noise ratio,	9.9 dB
$(SNR)_{IF} = \frac{E_b}{N_o} \cdot \frac{R_b}{B_{IF}}$	
Specified margin	6.00 dB
Total IF signal to noise ratio, $(SNR)_{IF}$	15.9 dB

50150-9T

2. Link Performance Summary

2.6 LINK DESIGN CONTROL TABLES

The Design Control Tables shown are for the experimental and deployed LDRLs, respectively. These are for the most critical communication situation — the shuttle to Molniya link (maximum range 46720 km). The experimental LDRL is distinguished from the deployed LDRL by its smaller receiver aperture diameter (16.51 cm, due to the present receiver optomechanical subsystem brassboard) and the correspondingly reduced intermediate frequency bandwidth (219 MHz) required to maintain $(\text{SNR})_{\text{IF}} = 15.9$ dB. The Design Control Table expresses in logarithmic form the relationship

$$(\text{SNR})_{\text{IF}} = \frac{P_T \eta_T G_T \eta_S G_R \eta_R \eta \eta_N}{h \nu_c B_{\text{IF}}}$$

where

P_T = modulated laser output power

η_T = transmitter loss

G_T = transmitter aperture gain

η_S = space loss

G_R = receiver aperture gain

η_R = receiver loss

η = detector quantum efficiency

h = Planck's constant

ν_c = optical carrier frequency

B_{IF} = intermediate frequency bandwidth

and $\eta_N = (\text{SNR})_{\text{IF}} / (\text{SNR})_{\text{IF ideal}}$ is the detector noise degradation from ideal due to all noise mechanisms.

LINK DESIGN CONTROL TABLE (EXPERIMENT)

	NOMINAL	FAV. TOL.	ADV. TOL.
TRANSMITTER PARAMETERS			
MODULATED LASER OUTPUT POWER(1.00W)	.00	.000	.000
BEAM SPLITTER LOSS.....	-.22	.023	-.023
COLLIMATING LENS LOSS.....	-.09	.009	-.009
DIPLEXER LOSS.....	-.41	.043	-.043
BEAM PREEXPANDER LOSS.....	-.44	.090	-.092
IMAGE MOTION COMPENSATOR LOSS.....	-.22	.022	-.022
RELAY MIRRORS LOSS.....	-.22	.045	-.046
BEAM EXPANDER LOSS.....	-.44	.090	-.092
POINTING MIRROR LOSS.....	-.11	.022	-.022
OBSCURATION LOSS (GAMMA=.417).....	-3.49	.000	.000
POINTING LOSS.....	.00	.000	-.079
IDEAL APERTURE GAIN(180M APERTURE)	94.54	.000	.000
PATH PARAMETERS			
SPACE LOSS (R=46720, KM).....	-274.87	.000	.000
RECEIVER PARAMETERS			
IDEAL APERTURE GAIN(165M APERTURE)	93.79	.000	.000
OBSCURATION LOSS (GAMMA=.200).....	-.18	.000	.000
IMAGE MOTION COMPENSATOR LOSS.....	-.46	.048	-.049
LOCAL OSCILLATOR DIPLEXER LOSS.....	-.04	.004	-.004
BEACON DIPLEXER LOSS.....	-.13	.013	-.013
OPTICS REFLECTANCE LOSSES.....	-.44	.086	-.092
HETERODYNE DETECTION LOSS.....	-1.85	.225	-.237
DETECTOR NOISE DEGRADATION.....	-.47	.084	-.208
PLANCK'S CONSTANT.....	331.78	.000	.000
CARRIER FREQUENCY,DB(HZ).....	-134.52	.000	.000
DETECTOR QUANTUM EFFICIENCY.....	-2.22	.000	-.792
IF BANDWIDTH,DB(HZ) (219,MHZ).....	-83.41	.000	.000
IF SIGNAL TO NOISE RATIO.....	15.89	.805	-1.825

50150-107

LINK DESIGN CONTROL TABLE (DEPLOYED)

	NOMINAL	FAV. TOL.	ADV. TOL.
TRANSMITTER PARAMETERS			
MODULATED LASER OUTPUT POWER(1.00W)	.00	.000	.000
BEAM SPLITTER LOSS.....	-.22	.023	-.023
COLLIMATING LENS LOSS.....	-.09	.009	-.009
DIPLEXER LOSS.....	-.41	.043	-.043
BEAM PREEXPANDER LOSS.....	-.44	.090	-.092
IMAGE MOTION COMPENSATOR LOSS.....	-.22	.022	-.022
RELAY MIRRORS LOSS.....	-.22	.045	-.046
BEAM EXPANDER LOSS.....	-.44	.090	-.092
POINTING MIRROR LOSS.....	-.11	.022	-.022
OBSCURATION LOSS (GAMMA=.417).....	-3.49	.000	.000
POINTING LOSS.....	.00	.000	-.079
IDEAL APERTURE GAIN(180M APERTURE)	94.54	.000	.000
PATH PARAMETERS			
SPACE LOSS (R=46720, KM).....	-274.87	.000	.000
RECEIVER PARAMETERS			
IDEAL APERTURE GAIN(1296M APERTURE)	98.85	.000	.000
OBSCURATION LOSS (GAMMA=.200).....	-.18	.000	.000
IMAGE MOTION COMPENSATOR LOSS.....	-.46	.048	-.049
LOCAL OSCILLATOR DIPLEXER LOSS.....	-.04	.004	-.004
BEACON DIPLEXER LOSS.....	-.13	.013	-.013
OPTICS REFLECTANCE LOSSES.....	-.44	.086	-.092
HETERODYNE DETECTION LOSS.....	-1.85	.225	-.237
DETECTOR NOISE DEGRADATION.....	-.47	.084	-.208
PLANCK'S CONSTANT.....	331.78	.000	.000
CARRIER FREQUENCY,DB(HZ).....	-134.52	.000	.000
DETECTOR QUANTUM EFFICIENCY.....	-2.22	.000	-.792
IF BANDWIDTH,DB(HZ) (704,MHZ).....	-88.48	.000	.000
IF SIGNAL TO NOISE RATIO.....	15.89	.805	-1.825

50150-117

2. Link Performance Summary

2.7 CONSTANTS USED IN DESIGN CONTROL TABLE CALCULATIONS

The table enumerates the system losses and other constants, along with associated tolerances, used in the Design Control Table calculations. The origin and significance of the losses are detailed in the Second Quarterly Report. The specified 1 watt output power represents the maximum modulated 10.6 μm laser sideband output power than can reasonable be anticipated at this time. The zero pointing error (and correspondingly zero pointing loss) assumes the implementation of the active point ahead compensation discussed in Section 3.

CONSTANTS USED IN LDRL LINK BUDGET CALCULATIONS

50150-12T

TRANSMITTER PARAMETERS	NOMINAL	FAV. TOL.	ADV. TOL.
MODULATED LASER OUTPUT POWER, DB(W)	1.00	0.00	0.00
BEAM SPLITTER LOSS, PERCENT	2.00	0.00	0.00
COLLIMATING LENS LOSS, PERCENT	2.00	0.00	0.00
DIPLEXER LOSS, PERCENT	0.00	0.00	0.00
BEAM FREE EXPANDER LOSS, PERCENT	0.00	0.00	0.00
IMAGE MOTION COMPENSATOR LOSS, PERCENT	4.00	0.00	0.00
RELAY MIRRORS LOSS, PERCENT	4.00	0.00	0.00
BEAM EXPANDER LOSS, PERCENT	0.00	0.00	0.00
POINTING MIRROR LOSS, PERCENT	2.00	0.00	0.00
POINTING ERROR, MICRORADIANS	0.00	0.00	0.00
POINTING LOSS, PERCENT	0.00	0.00	0.00
RECEIVER PARAMETERS			
IMAGE MOTION COMPENSATOR LOSS, PERCENT	10.00	0.00	0.00
LOCAL OSCILLATOR DIPLEXER LOSS, PERCENT	1.00	0.00	0.00
BEACON DIPLEXER LOSS, PERCENT	3.00	0.00	0.00
OPTICS REFLECTANCE LOSSES, PERCENT	0.00	0.00	0.00
HETERODYNE DETECTION LOSS, PERCENT	34.70	0.00	0.00
DETECTOR QUANTUM EFFICIENCY, PERCENT	60.00	0.00	0.00
DETECTOR GAIN	1.00	0.00	0.00
DETECTOR LOAD RESISTANCE, OHMS	50.00	0.00	0.00
DETECTOR DARK CURRENT, MICROAMPS	1.00	0.00	0.00
POSTAMPLIFIER NOISE TEMPERATURE, DEGREES K	350.00	0.00	0.00
LOCAL OSCILLATOR POWER, WATTS	0.00200	0.00	0.00
BACKGROUND RADIANCE, WATTS/30 MICRONS*STERADIAN	0.00100	0.00	0.00
DETECTOR FIELD OF VIEW, MICRORADIANS	49.46	0.00	0.00

2. Link Performance Summary

2.8 TRANSMITTER AND RECEIVER WEIGHT AND POWER TABULATIONS

These charts present weight and power tabulations for both the experimental (16.51 cm aperture) and deployed (29.57 cm aperture) LDRL receivers for a transmitter having an 18 cm aperture and a 1 watt output. This transmitter is common to both links. (Package A refers to the receiver which has the configuration of the OMSS. Package B has a configuration capable of hemispherical angular coverage and is described in detail in this report.) The tabulations are another output of the same Link Analysis program which generates the Design Control Tables. The weight and power modeling upon which the tabulations are based have been discussed in the First Quarterly Report.

TRANSMITTER WEIGHT AND POWER TABULATION

IF BANDWIDTH, MHZ	
OPTIMIZED VALUES	
PACKAGE B (TRANSMITTER) ANTENNA DIAMETER, M	.1800
PACKAGE A (RECEIVER) ANTENNA DIAMETER, M	.2957
TRANSMITTER OUTPUT POWER, WATTS	1.0000
TRANSMITTER EFFICIENCY, PERCENT	1.0000
PACKAGE B WEIGHT TABULATION, POUNDS	
STRUCTURE WEIGHT	24.37
OPTICAL TELESCOPE WITH MOUNTINGS	8.15
SIGNALS, MOTORS, AND STEERING MIRROR	9.72
SERVO ELECTRONICS	4.42
LASER, MODULATOR, AND MODULATOR DRIVER (1)	25.00
SERVO POWER CONDITIONING	7.33
OTHER POWER CONDITIONING	12.50
DIPLEXER AND MISCELLANEOUS OPTICS	3.06
LASER STABILIZATION ELECTRONICS	.40
BEACON DETECTOR AND POWER SUPPLY (1)	.58
BEACON RECEIVER OPTICS AND ELECTRONICS	.66
IMAGE MOTION COMPENSATION SUBSYSTEM	2.62
CABLES AND CONNECTORS	1.71
MISCELLANEOUS	10.05
PACKAGE B TOTAL WEIGHT	110.57
ASSOCIATED PRIME POWER SYSTEM WEIGHT	116.63
PACKAGE B ASSOCIATED WEIGHT BURDEN	227.21
PACKAGE B POWER TABULATION WATTS	
TRANSMITTER LASER INPUT POWER	100.00
TRANSMITTER ELECTRONICS POWER	76.00
POINTING SUBSYSTEM POWER	8.25
BEACON RECEIVER POWER	1.00
CONTROL PANEL POWER	10.00
PACKAGE B SYSTEM POWER	195.25

50150-15T

EXPERIMENTAL RECEIVER WEIGHT AND POWER TABULATION

50150-137

PACKAGE A WEIGHT TABULATION, POUNDS

STRUCTURE WEIGHT	10.97
OPTICAL TELESCOPE WITH MOUNTINGS	55.83
GIMBALS, MOTORS, AND STEERING MIRROR	10.31
SERVO ELECTRONICS	4.30
RECEIVER AND SIGNAL PROCESSING ELECTRONICS (1)	19.03
SERVO POWER CONDITIONING	6.60
OTHER POWER CONDITIONING	1.00
BEACON LASER (1)	1.00
LOCAL OSCILLATOR LASER (1)	1.00
DETECTOR AND DETECTOR COOLER	1.50
BEAM EXPANDER AND DEFOCUS MECHANISM	2.70
IMAGE MOTION COMPENSATION SUBSYSTEM	2.41
CABLES AND CONNECTORS	0.15
MISCELLANEOUS	0.98
PACKAGE A TOTAL WEIGHT	98.79
ASSOCIATED PRIME POWER SYSTEM WEIGHT	91.21
PACKAGE A ASSOCIATED WEIGHT BURDEN	190.00

PACKAGE A POWER TABULATION WATTS

LOCAL OSCILLATOR INPUT POWER	13.00
RECEIVER ELECTRONICS POWER	18.12
POINTING SUBSYSTEM POWER	7.40
BEACON TRANSMITTER POWER	100.00
CONTROL PANEL POWER	10.00
PACKAGE A SYSTEM POWER	148.52

DEPLOYED RECEIVER WEIGHT AND POWER TABULATION

50150-147

PACKAGE A WEIGHT TABULATION, POUNDS

STRUCTURE WEIGHT	30.48
OPTICAL TELESCOPE WITH MOUNTINGS	20.24
GIMBALS, MOTORS, AND STEERING MIRROR	12.31
SERVO ELECTRONICS	4.33
RECEIVER AND SIGNAL PROCESSING ELECTRONICS (1)	20.10
SERVO POWER CONDITIONING	8.66
OTHER POWER CONDITIONING	12.00
BEACON LASER (1)	1.00
LOCAL OSCILLATOR LASER (1)	2.00
DETECTOR AND DETECTOR COOLER	3.50
BEAM EXPANDER AND DEFOCUS MECHANISM	8.70
IMAGE MOTION COMPENSATION SUBSYSTEM	9.08
CABLES AND CONNECTORS	2.66
MISCELLANEOUS	13.30
PACKAGE A TOTAL WEIGHT	146.35
ASSOCIATED PRIME POWER SYSTEM WEIGHT	97.42
PACKAGE A ASSOCIATED WEIGHT BURDEN	243.77

PACKAGE A POWER TABULATION WATTS

LOCAL OSCILLATOR INPUT POWER	13.00
RECEIVER ELECTRONICS POWER	26.28
POINTING SUBSYSTEM POWER	10.87
BEACON TRANSMITTER POWER	100.00
CONTROL PANEL POWER	10.00
PACKAGE A SYSTEM POWER	160.16

3. Acquisition and Tracking

3.1 SUMMARY

The systems analysis tasks for the first phase of the LDRL transmitter project are given in the table. The features of the overall servo system were first defined. The selected concept involved several control loops. Following this, an analysis of several acquisition concepts was completed. Because of the large telescope field of view compared to the detector field of view and because of the target rates involved, acquisition presents a difficult problem. Next, the orbital motion of the Shuttle relative to the ground station was analyzed to determine gimbal motions, target motions, and coordinate conversions. Finally, based on the above analysis and other program constraints, the servo requirements were defined

SYSTEMS ANALYSIS TASKS

- | |
|--|
| Conceptual design of overall servo system |
| Analysis of acquisition concepts |
| Analysis of orbital motions |
| • Target motion, gimbal motion, and coordinate conversions |
| • Lead angle requirements |
| Definition of servo requirements |
| • Acquisition mode |
| • Coarse track mode |
| • Fine track mode |
| • Point ahead requirements |

50150-167(U)

PRECEDING PAGE BLANK NOT FILMED

3. Acquisition and Tracking

3.2 Requirements

3.2.1 SHUTTLE TO GROUND LINK

The minimum acquisition requirements for the Shuttle to ground link are given in the opposite figure. It is assumed for this link that the Shuttle pointing uncertainty is $\pm 0.5^\circ$. This is the same as the field of view of the optics. Therefore, the target at the start of the acquisition phase can theoretically be brought within the field of view by commanding the gimbals to the required angles.

Two cases are considered. In the first it is assumed that part of the target motion is compensated through gimbal commands such that the resultant relative motion is only 0.09 deg/sec. For the second case, it is assumed that the relative target motion is not taken out by the gimbals; the gimbals are simply commanded to azimuth and elevation positions through which the target will pass at the time the spacecraft is 60° from zenith.

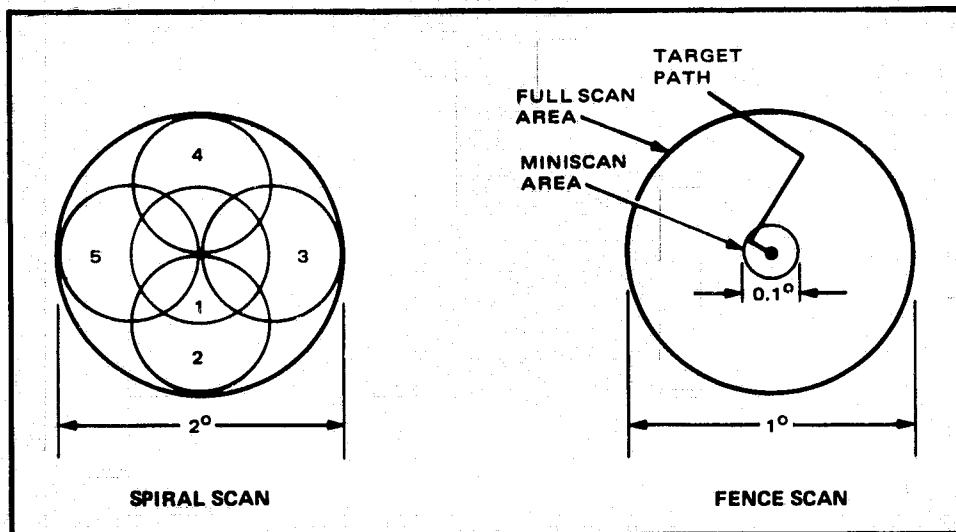
For the first case, a spiral scan using the image motion compensator (IMC) is used to cover the entire 1° field. A simple five-position gimbal scan is superimposed on the IMC scan to add a factor of two margin to the IMC field of view. For the second case a circular fence scan is used to effect scanning in essentially one dimension. The Shuttle motion will bring the beacon across the detector.

The postdetection bandwidth in the table refers to the optimum filter bandwidth to detect the acquisition pulse. This pulse has a width which in turn depends on the scan velocity through the field of view.

SHUTTLE TO GROUND LINK ACQUISITION REQUIREMENTS

Parameter	Spiral Scan	Fence Scan
	Target Velocity = 0.09 deg/sec	Target Velocity = 0.25 deg/sec
Scan frequency, Hz	54	150
Postdetection bandwidth, kHz	111	309
Frame telemetry, sec	6	4
Line resolution, μ rad	29	29
Number of lines	300	300

50150-18T



50150-17

SHUTTLE TO GROUND LINK ACQUISITION REQUIREMENTS

3. Acquisition and Tracking

3.2 Requirements

3.2.2 SHUTTLE TO MOLNIYA

The figure shows the acquisition requirements for the Shuttle to Molniya link. As is the previous case, a spiral scan covering the entire 1° field of view is used to locate the target, and a miniscan covering a $\pm 0.05^\circ$ field of view is used to actually acquire the target.

The target velocity of 0.015 deg/sec is based on the assumptions that 1) 90 percent of the real target motion of 0.05 deg/sec can be removed through a ground commanded gimbal control program and 2) the base motion of the satellite will be less than 0.01 deg/sec. For the miniscan, the maximum target velocity that can be accommodated is increased to 0.08 deg/sec. This is because of the higher scan frequency employed for that mode.

One of the objectives in devising the acquisition scheme was to reduce the postdetection bandwidth below 30 kHz, in order to maintain adequate detection signal-to-noise ratio. As can be seen, the required bandwidths are well within these constraints.

SHUTTLE TO MOLNIYA LINK ACQUISITION REQUIREMENTS

Parameter	Coarse Scan	Miniscan
Target velocity, deg/sec	0.015	0.08
Scan frequency, Hz	9	50
Type scan	Spiral	Spiral
Postdetection bandwidth, kHz	18.4	4.7
Frame time, sec	33	0.6
Line resolution, μ rad	29	29
Number of lines	300	30

50150-19T

3. Acquisition and Tracking

3.2 Requirements

3.2.3 IMAGE MOTION COMPENSATOR

The IMC requirements are given in the table for the both the Shuttle to ground link and Shuttle to Molniya link. These requirements are based on the acquisition schemes discussed in the last two topics.

The mirror size, as discussed in the optical design presentation, is the smallest value that is consistent with the design requirements. The angular deflection is determined by the telescope magnification (7) and field of view ($\pm 0.5^\circ$). The required servo bandwidth is determined by the IMC scan speed. For the Shuttle to ground link this can vary from 100 to 175 Hz.

The angular readout accuracy is determined by the angular subtense of the received beam (58 μ rad). The linearity is required over a $\pm 0.1^\circ$ field. The resolution is based on the fine track requirements.

IMC REQUIREMENTS

Parameter	Shuttle to Ground Link	Shuttle to Molniya Link
Mirror size, in.	1 x 1.4	1 x 1.4
Angular deflection, deg	± 1.75	± 1.75
Servo bandwidth, Hz	100 to 175	100
Position readout requirements		
• Accuracy, μrad	± 15	± 15
• Linearity, %	± 0.8	± 0.8
• Resolution, μrad	± 2.5	± 2.5

50150-2281

3. Acquisition and Tracking

3.2 Requirements

3.2.4 GIMBAL SERVO

The table shows the gimbal servo requirements. These requirements are based on the Shuttle to ground link, which was selected as a servo baseline because the tracking dynamics are generally more stringent than for the Shuttle to Molniya link. The maximum acquisition target velocity is based on the assumption that acquisition will take place before a zenith angle of 60° . The field of view is 80° each side of zenith. The allowed angular sector to acquire is the sector from 80° to 60° zenith in a 500 km orbit. This sector is traversed in approximately 2 minutes.

The base motion required is the expected Shuttle base motion. The maximum gimbal angles and rates are for a 500 km orbit and for a ground station on the equator. These represent worst case conditions.

The servo bandwidth is based on the required pointing rates during the acquisition mode.

GIMBAL SERVO REQUIREMENTS

Operational modes	Acquisition (search and pointing)
	Coarse track
Target data	
Maximum target velocity	0.8 deg/sec
Acquisition target velocity	0.25 deg/sec
Maximum target acceleration	0.007 deg/sec ²
Time in field of view	10 min
Allowable acquisition time	2 min
Base motion	
Short term	0.01 deg/sec
Long term	0.1 deg/hr
Gimbal motion	
Roll angle	±68°
Roll rate	0.2 deg/sec
Pitch angle	±68°
Pitch rate	0.8 deg/sec
Gimbal control requirements	
Bandwidth	10 Hz
Coarse track accuracy	±0.1°
Pointing accuracy	±0.02°

50150-211

3. Acquisition and Tracking

3.2 Requirements

3.2.5 FINE TRACK AND LEAD ANGLE CORRECTOR

The requirements for the fine track loop and lead angle corrector (point ahead device) are given in the table. The fine track bandwidth is chosen great enough to minimize interaction with the gimbal control loop and also to stabilize the image to $\pm 5 \mu\text{rad}$ against residual target motion not removed by the gimbal loop. The signal-to-noise ratio requirement is based on maintaining $\pm 5 \mu\text{rad}$ angular noise with a $10 \mu\text{rad}$ amplitude modulation of a $58 \mu\text{rad}$ beamwidth.

The same device used for nutating the received beam (to develop an error signal) is used to impart the required lead angle. The amplitude of the required angular deflection is based on the magnification at that point, 45, and, upon the required beam deflection in object space, $84 \mu\text{rad}$. The specified linearity is good enough to essentially eliminate that source of error from the lead angle correction. The bandwidth is based on a nutation scan frequency of 150 Hz.

REQUIREMENT SUMMARY

FINE TRACK REQUIREMENTS

Bandwidth	50 Hz
Total track error*	10 μ rad
Noise error	• 5 μ rad
Dynamic error	• 5 μ rad
Signal-to-noise ratio	20 dB
Dynamic range*	$\pm 0.1^\circ$

LEAD ANGLE CORRECTOR/BEAM NUTATOR

Conical scan amplitude*	15 μ rad
Conical scan frequency	150 Hz
Corrector bandwidth	300 Hz
Angular deflection	0.214°
Pickoff linearity	1%
Aperture size	5 mm

*Referred to object space.

50150-22T

3. Acquisition and Tracking

3.3 SYSTEM BLOCK DIAGRAM

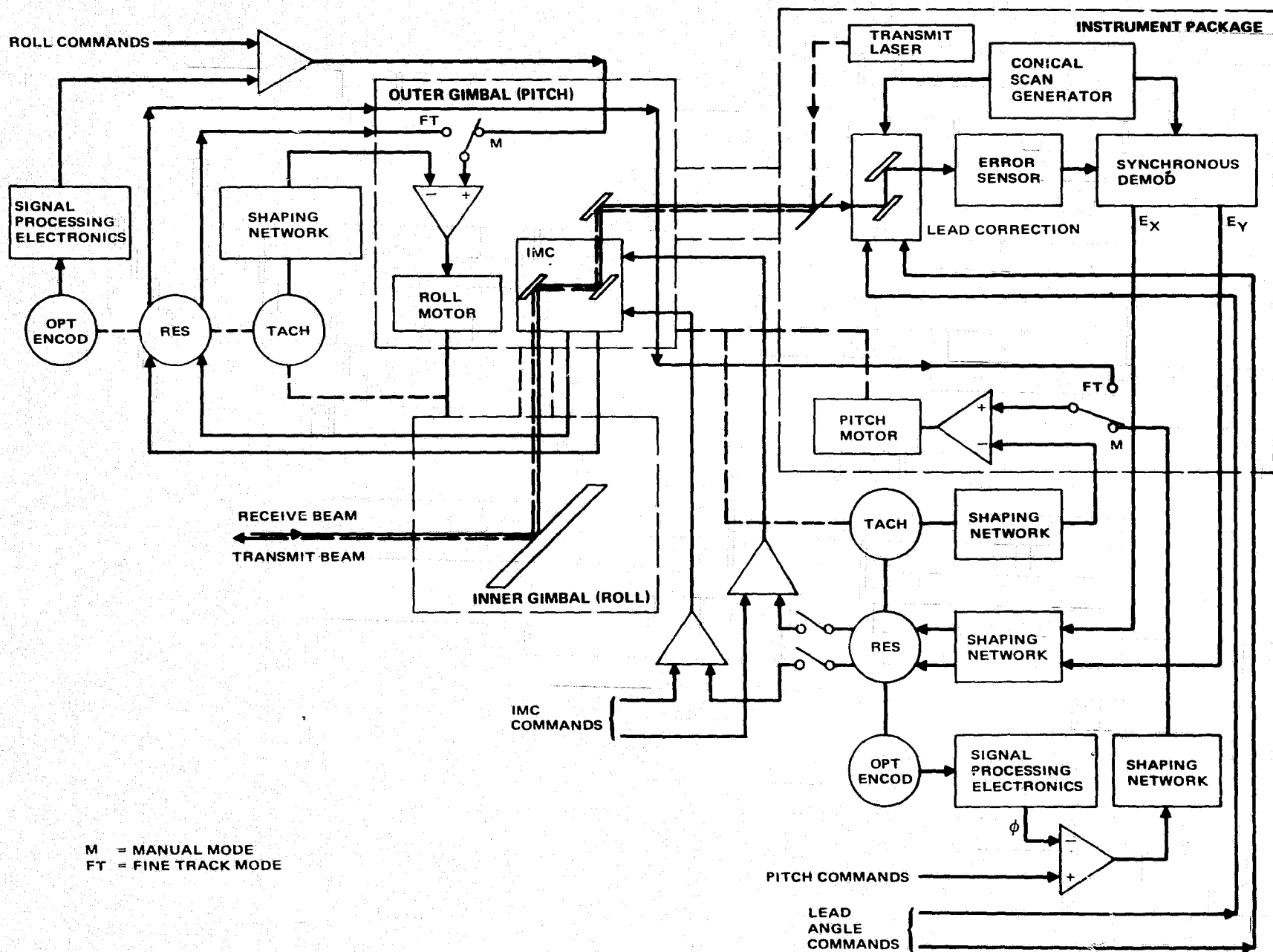
The acquisition and tracking servo loop block diagram is shown in the figure. The system uses a multiloop concept in which a wideband, fine track loop maintains the required track accuracy while a coarse loop maintains the fine loop actuator within its bounds. The actuator for the fine loop is the image motion compensator (IMC), which is located on the outer gimbal. Motion of the IMC affects the X-Z components of error as measured at the error sensor.

The error sensor uses the same beam dithering/synchronous demodulation technique that is used in the NASA optomechanical subsystem receiver. Error signals from the sensor are resolved into the proper components for application to the IMC actuator.

The coarse track loop for one axis consists of the IMC angle transducer, necessary frequency shaping (not shown), resolver, gimbal drive motor, and gimbal dynamics. The loop is completed through the laser beam and the laser detector. A track loop is used for damping.

Both the IMC actuator and gimbal control loops are subject to external control in the manual mode (M) as indicated in the figure. The gimbal control will be used during acquisition to point the gimbals to the expected target position, and at the same time the IMC will execute a command search pattern.

Finally, for lead angle correction (point ahead) a special actuator (which doubles as a nutator for beam dithering) is provided. The required angle will be continuously commanded during flight, either from the ground, or from an onboard program which is addressable from the ground through a command link, or through a servo loop which encompasses the other terminal.



4. Optomechanical Subsystem Design

4.1 SUMMARY

The primary effort during this reporting period was concentrated on completing the layout to the greatest degree possible. The goal was that of designing a model that could be fabricated in a most cost effective manner while maintaining optical performance. Package weight was allowed to increase since this is not a critical item for the Shuttle.

The materials/cost tradeoff selected beryllium for the telescope and optics, and 400 series (17-7 or 17-4 Ph) stainless steel for other components. This selection provides thermal expansion matching of the critical components.

The telescope will be designed with separable and bench adjustable sub-assemblies for ease of alignment and adjustment. The IMCs and field stop will be alignable as a unit prior to installation into the telescope structure. The outer gimbal folding mirror is supported at three points and is adjustable by dual threaded jackscrews at those locations. The inner gimbal pointing mirror is hard mounted to its housing, but adjustable at the housing/bearing interface.

The telescope reflective optics are alignable by the use of existing tooling created for the optomechanical subsystem 10 μ m receiver. This tooling is available. The entire telescope, inner and outer gimbals and relay lens alignment mechanisms, is accessible and can be aligned as a total unit.

A preliminary analysis of the outer gimbal has been conducted to review the effect of testing the system in a 1 g environment. In order to keep breakaway friction to a minimum, a torque limit about the bearings of 10 to 15 in-oz torque was used as an upper bound. The results for the 1g field are as follows:

<u>Preload, lb</u>	<u>Minimum "Sag" Angle, μrad</u>	<u>Maximum "Sag" Angle, μrad</u>	<u>Torque, in-oz</u>
75	29	53	10
110	25	46	15

Both values of sag and torque are deemed acceptable at this time. If the sag due to the 1 g field should become a problem, an off loading device could be added.

Based upon the launch vibration information currently available for experiment mounting interfaces, structural dynamics analysis has shown a static equivalent load criteria of 65 g's is possible. This requires a beryllium gauge thickness for the telescope structure of 0.050 inch minimum. With such a structure, the resultant 1 g model sag will be less than 5 μ rad.

PRECEDING PAGE BLANK NOT FILMED

4. Optomechanical Subsystem Design

4.2 Gimbal/Structure Layout Review

4.2.1 GENERAL OPERATIONAL CONCEPT AND PROGRAM GOALS

The documentation of the layout phase is the subject of this review. The review encompasses more than will be included in the pending optical brassboard phase to assure an integrated design suitable for upgrade to a flyable experiment.

OPTOMECHANICAL PACKAGE

50150-24T

TWO-STAGE BEAM POINTING SYSTEM

- Motor driven gimbals for coarse pointing
- IMCs for search/scan and fine pointing

LAYOUT PHASE

- Establish optomechanical subsystem requirements
- Define configuration
- Provide basis for detail drawing preparation

BRASSBOARD PHASE

- Fabricate and assemble preliminary engineering model
- Telescope, pre-expander, structure, and gimbal only
- Capable of future upgrade to full model
- Conduct open loop operation
- Perform open end checkout on optical bench for alignment

FUTURE EFFORTS

- Define, develop, and construct IMCs
- Provide servo system and electronics
- Include nutating/lead angle device
- Add acquisition optics hardware
- Package detector and communication hardware
- Possibly fly as an experiment

1

4. Optomechanical Subsystem Design

4.2 Gimbal/Structure Layout Review

4.2.2 SYSTEM PARAMETERS FOR UPGRADED FLYABLE EXPERIMENT

The system parameters are given in the table. The more pertinent items are:

- 1) The small restrictions from full hemispheric coverage due to a two-axis system
- 2) The requirements for Shuttle inversion when changing from Shuttle to ground to Shuttle to Molniya links
- 3) The gimbal coarse pointing accuracy of $\pm 0.02^\circ$ is an achievable design goal. Actual requirement is closer to $\pm 0.05^\circ$. If hardware costs to achieve $\pm 0.02^\circ$ become excessive, this could be relaxed.
- 4) The acquisition field of view and IMC mirror size require an angular excursion range and load carrying capacity in excess of the existing GT&E PBM-8G IMCs. Achieving the required value will eventually necessitate the development of a new IMC.

LDRL TRANSMITTER SYSTEM PARAMETERS

50150-25T

Parameter	Value	Remarks
Telescope tracking field	Near hemisphere	15° from X-Y plane in the Y-Y direction is field limit to avoid gimbal lock with the two-axis system
Range *	185 to 46,720 km	Vehicle inversion required to shift between Shuttle to ground and Shuttle to elliptical links
Gimbal coarse pointing accuracy	±0.02°	
Output clearance diameter	18.5 cm	Unobstructed for full acquisition field of view (measured 17 cm from optical centerline)
f number (primary)	f/1.5	
Acquisition field of view**	±0.5°	
Tracking rate (maximum)	0.8 deg/sec	
Transmit signal	10.6 μm	
Receive beacon	10.6 μm	0.9 μm is a possible alternate
Magnification	7.086	
IMC mirror size**	2.5 x 3.6 cm	Elliptical shape

*For information only.

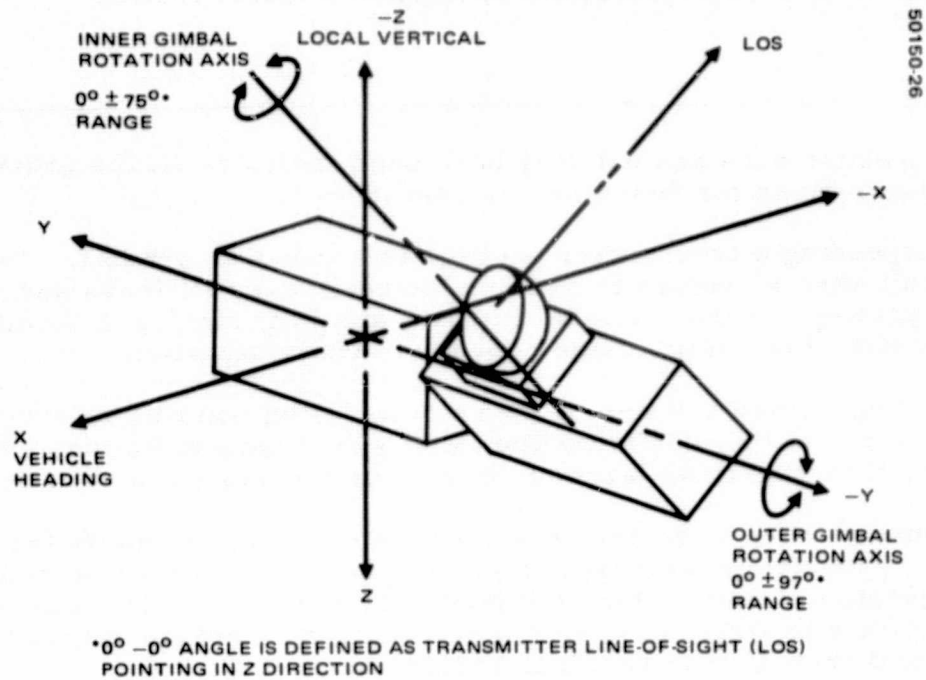
**These values are design goals and require subsequent development of an IMC device beyond the scope of the preliminary engineering model.

4. Optomechanical Subsystem Design

4.2 Gimbal/Structure Layout Review

4.2.3 TRANSMITTER COORDINATE SYSTEM

The opposite figure shows the unit orientation in space and defines the angular coverage.



TRANSMITTER COORDINATE SYSTEM

4. Optomechanical Subsystem Design

4.2 Gimbal/Structure Layout Review

4.2.4 OVERALL OPTOMECHANICAL SUBSYSTEM PACKAGING

The telescope axes and pointing have been indicated on the previous figure. Alternate configurations for Spacelab considered were:

1) Suspending a transmitter package in a two-axis gimbal. This would require a complicated structure to provide the necessary stiffness and would have much greater package volume, gimbal inertia, and heat sinking difficulties. It would have the advantage of no image coordinate transformation.

2) Having a fixed telescope, then manipulating pointing mirrors (cleostats) to direct the beam. In this configuration IMCs would have to be located far from the main expander, thus requiring larger mirrors for the same effective aperture size.

DC torque motors were selected over stepper motors due to the inability of a stepper motor system to meet output angle rate requirements while satisfying operational requirements of small step size (0.000286 deg/step). Direct drive was chosen over an off-axis drive in order to achieve good tracking resolution with a stiff drive system free of gear backlash problems.

LDRL TRANSMITTER MODEL

50150-277

GENERAL ARRANGEMENT CONSIDERATIONS

- Laser transmitter must be heat sunk
- Minimize weight and inertia of gimballed elements for lightweight and low power
 - Coarse gimbal for wide coverage
 - Fine (IMC) for high frequency response and accuracy of laser beam
- Telescope gimballed to minimize folding mirror size with large angle requirement

DIRECT DRIVE MOTOR SELECTED

- Ensures high rate and resolution
- Provides minimum backlash
- Meets wear life requirement of low altitude orbit

4. Optomechanical Subsystem Design

4.2 Gimbal/Structure Layout Review

4.2.5 MECHANICAL DESIGN CONSIDERATIONS FOR TESTING IN A GRAVITATIONAL FIELD AND OVERALL MECHANICAL REQUIREMENTS

The stiffness and the bearing friction parameters of the optomechanical structure are related. Alignment and bench testing of the completed assembly will be accomplished by resting the unit on the surface which is normally mounted to the spacecraft. This will leave the rotatable telescope overhanging and will cause a sag due to the 1 g earth gravitational field. Stiffening the bearing suspension system to minimize this sag results in higher bearing friction torques. Therefore a compromise design was selected with performance values given in the table. Should the value of optical beam deflection due to the sag be intolerable, an off loading device could be incorporated as part of the bench setup. In any event, the inner gimbal will have to be counterbalanced to prevent mechanical instability in a 1 g field.

LDRL TRANSMITTER MODEL REQUIREMENTS

50150-28T

Parameter	Requirement	Method of Satisfaction	Validation Status
Gimbal freedom	Inner $\pm 75^\circ$ Outer $\pm 97^\circ$	Build in stops	Design layout and test
Rate (maximum)	0.08 deg/sec	DC torque motor	Excess capability
Stiffness	53 μ rad in 1 g field	Bearing preload spring	Analysis
Bearing friction	≈ 10 to 15 in-oz	Bearing preload spring	Analysis complete
Weight	Minimum	Cost/weight/performance	Tradeoff (estimate 50 lb)
Temperature range	Unknown	Estimate 20° to 100° F	Compatible materials
Vibration	Unknown at transmitter mounting interface	Estimate 65 g static equivalent	Dynamics/stress review
Future use	Shuttle flight experiment	Upgradeable in future	Material selection

4. Optomechanical Subsystem Design

4.2 Gimbal/Structure Layout Review

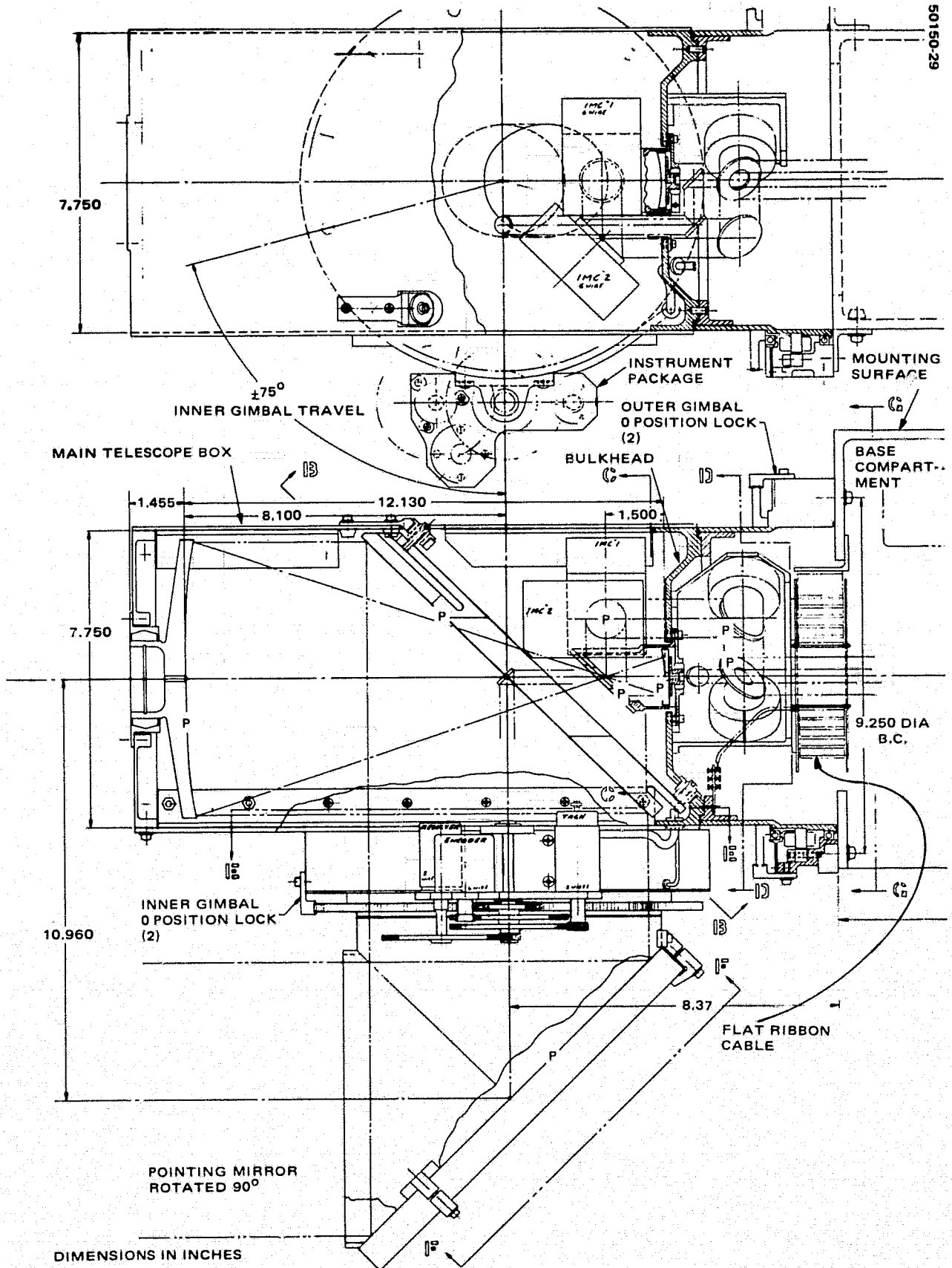
4.2.6 GENERAL ARRANGEMENT OF GIMBALS AND OPTICS

In the optomechanical subsystem, several subassemblies are formed. A modular approach has been used. These are indicated in the figure as the motor/bearing packages (one per axis), the instrument cluster (one per axial), the secondary folding mirror package, the IMC/field stop package, the folding mirrors for directing the beam to the base centerline, and the acquisition beam bypass. The optical components are all aligned as subassemblies and then the subassemblies are integrated into and aligned in the main package.

The materials used are:

- 1) Beryllium for all mirrors (marked p in the figure) and for the basic telescope box.
- 2) Stainless steel, series 400, for the beryllium box base bulkhead, the motor/bearing subassemblies, the inner gimbal structure, mirror subassemblies, and alignment details. This stainless series is chosen for its thermal expansion coefficient which is compatible with beryllium.
- 3) Aluminum for the base compartment structure and for the instrument mounting bracket and gears. Aluminum is chosen for its light weight, for its heat sinking capability, and for its relative low cost.

The "0" position locks are for ground use only and are removed for operation. They lock the rotation by seizing the main gear attached to each motor bearing package. Cabling across the outer gimbal axis is required for the inner gimbal motor control, for instruments, and for the two IMCs.



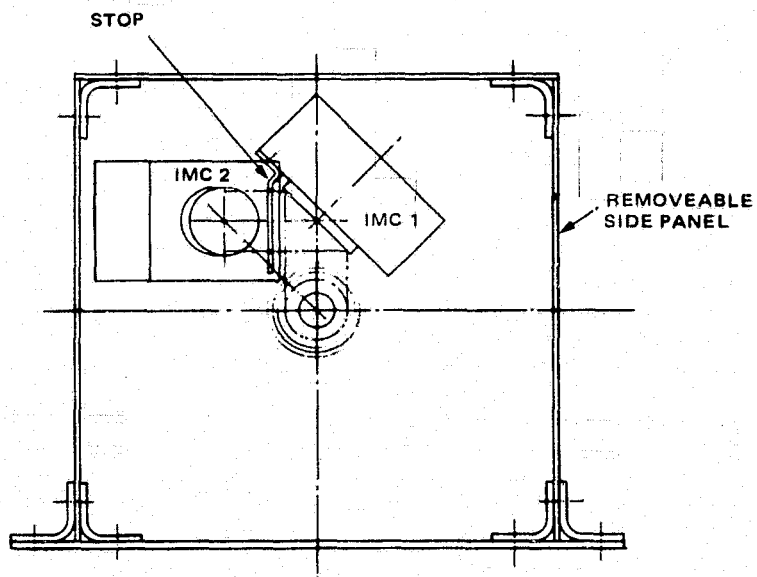
GENERAL ARRANGEMENT OF GIMBAL AND OPTICS

4. Optomechanical Subsystem Design

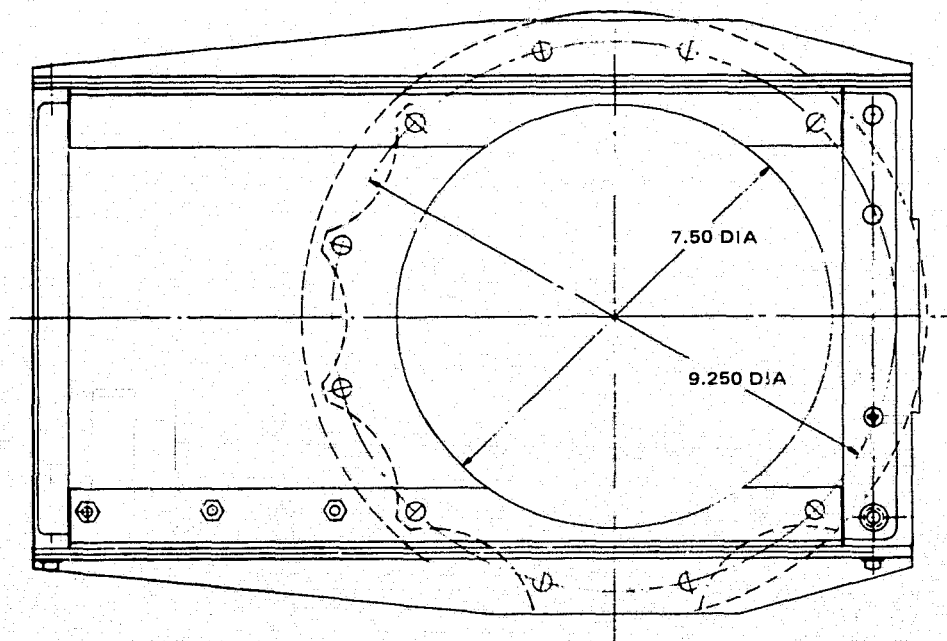
4.2 Gimbal/Structure Layout Review

4.2.7 BERYLLIUM TELESCOPE BOX STRUCTURE

The side panel indicated in the figure is removable for installation of the mirrors and other subassemblies. All joints, except for this removable panel, are bonded (with tack bolts) for structural integrity.



VIEW C - C



VIEW D - D

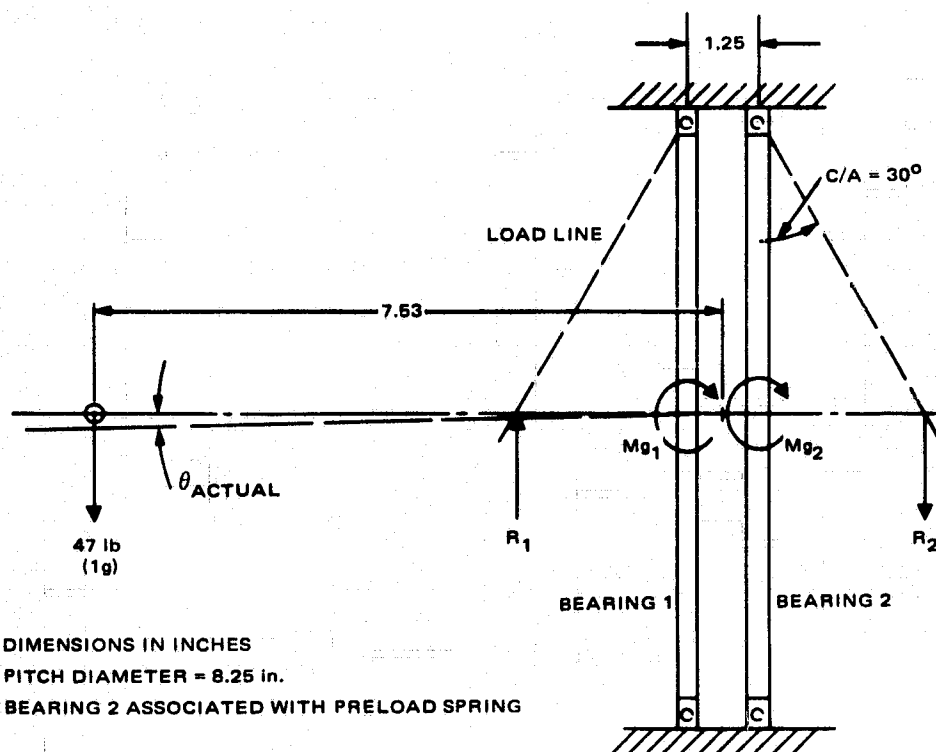
BERYLLIUM TELESCOPE BOX STRUCTURE

4. Optomechanical Subsystem Design

4.2 Gimbal/Structure Layout Review

4.2.8 BEARING ANALYSIS

The figure shows distances and force vectors involved in the bearing analysis. The analysis was performed by a Hughes computer program. Sag results are indicated in the figure.



BEARING PRELOAD, lb	MINIMUM 1g SAG, μrad	MAXIMUM 1g SAG, μrad	BREAKAWAY TORQUE, in-oz
75	29	53	10
110	25	46	15

LDRL TRANSMITTER MODEL BEARING ANALYSIS

4. Optomechanical Subsystem Design

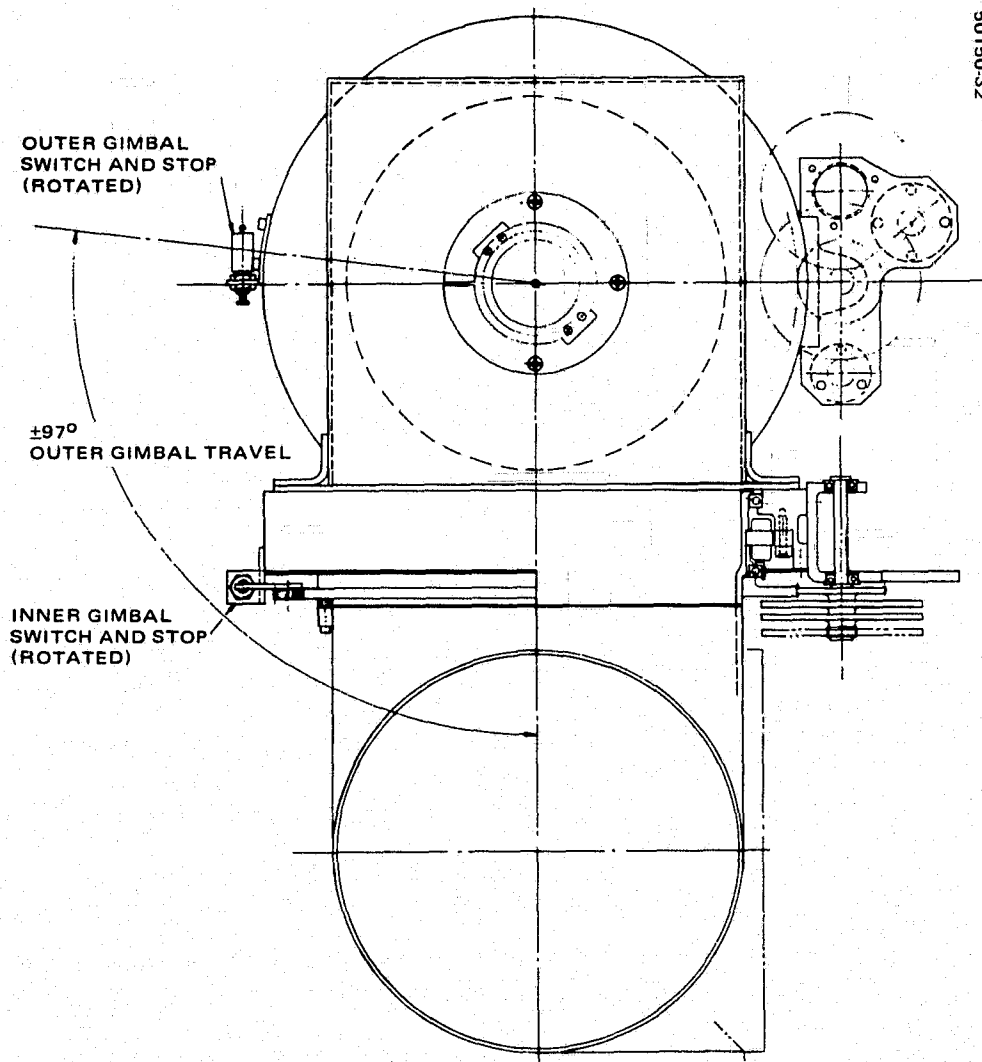
4.2 Gimbal/Structure Layout Review

4.2.9 END VIEW OF GIMBAL PACKAGE

The figure is an end view of the gimbal package showing instrument gear packages and switch at one end of travel for each axis. The purpose of the switch is to provide an electrical reference for position register initialization at unit turn-on.

Also shown in the upper portion of the figure is the end view of the primary focusing mirror adjustable mount. This interface duplicates that used on the previously assembled OMSS receiver and allows use of the same detail drawings.

50150-32



END VIEW OF GIMBAL PACKAGE

4. Optomechanical Subsystem Design

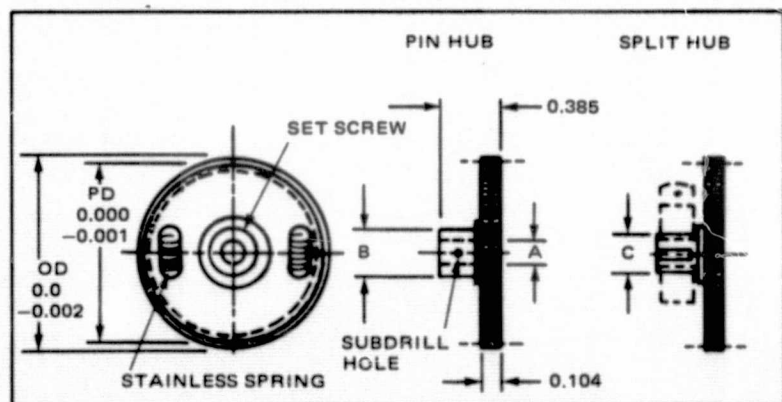
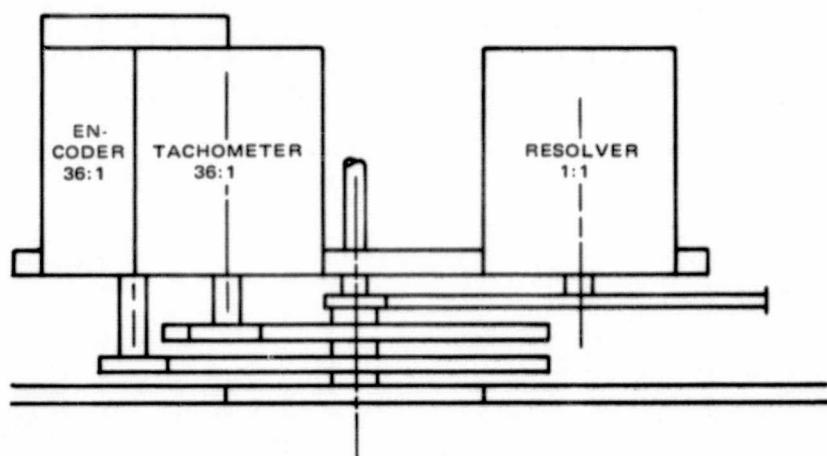
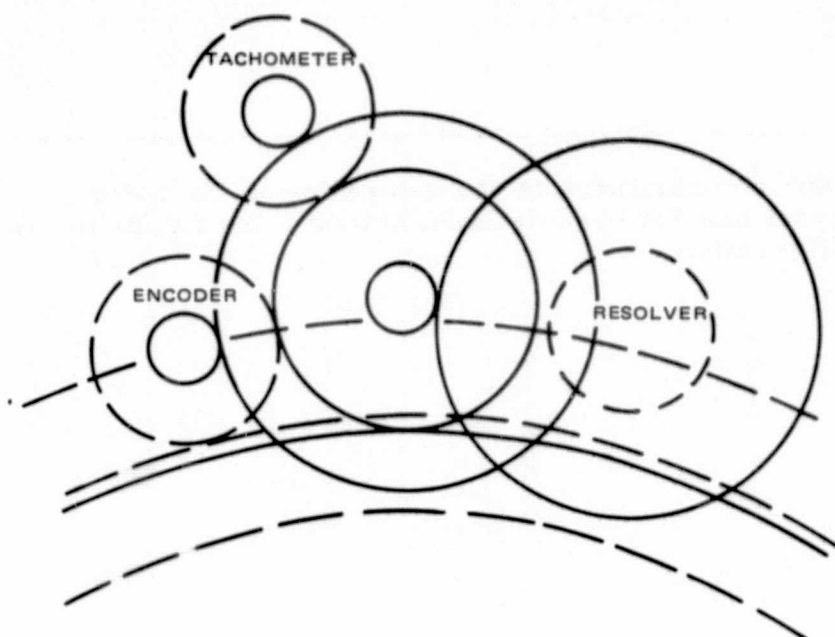
4.2 Gimbal/Structure Layout Review

4.2.10 INSTRUMENT GEARING ARRANGEMENT

The figure of the instrument gearing arrangement shows the operation of the components and the details of the standard antibacklash gears used in each mesh. Instrument items and their functions are:

- 1) Tachometer - This unit is geared 36:1 and is used for motor servo control. The indicated placement of the tachometer saves considerable cost, weight, and volume as opposed to a large item housed next to the motor.
- 2) Encoder - This unit is geared 36:1 and is used for position and pointing control. An optical encoder, 1000 counts per turn, placed here would yield a resolution of 0.01° .
- 3) Resolver - This unit is geared 1:1 and is used for coordinate transformation between the fixed detector and the rotating image.

In the final system, using the electronic components now available, only the encoder is required to achieve all three of the above functions. However, the brassboard unit will contain a tachometer, an encoder, and a resolver. This will permit independent access to each function for bench checkout while avoiding the necessity for design and fabrication of special electronics. The resolver and tachometer might well be eliminated in the final model.



MATERIAL

GEARS - 303 STAINLESS STEEL
2024-T4 ALUMINUM

HUBS - 303 STAINLESS STEEL

BORE	A	B	C	SET SCREW
1/8	0.1248	0.31	0.188	2-56
3/16	0.1873	0.37	0.250	4-40
1/4	0.2498	0.50	0.312	6-32

ANTIBACKLASH GEARS

INSTRUMENT GEARING ARRANGEMENT

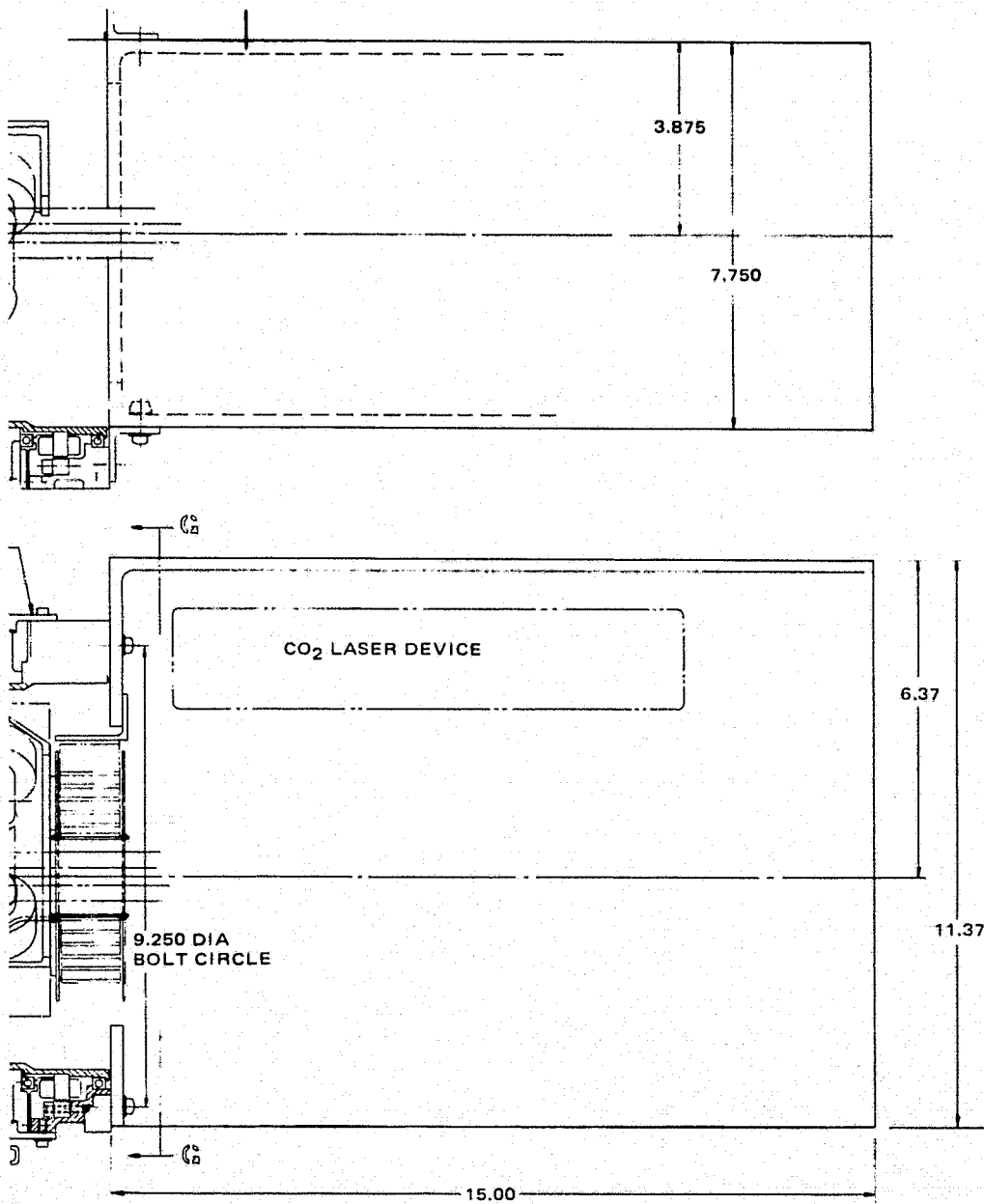
4. Optomechanical Subsystem Design

4.2 Gimbal/Structure Layout Review

4.2.11 BASE COMPARTMENT

The optical path enters the compartment on the centerline of the outer gimbal. At present the base layout has not been defined; however the figure in the next topic shows a possible configuration.

50150-34



DIMENSIONS IN INCHES

BASE COMPARTMENT

4. Optomechanical Subsystem Design

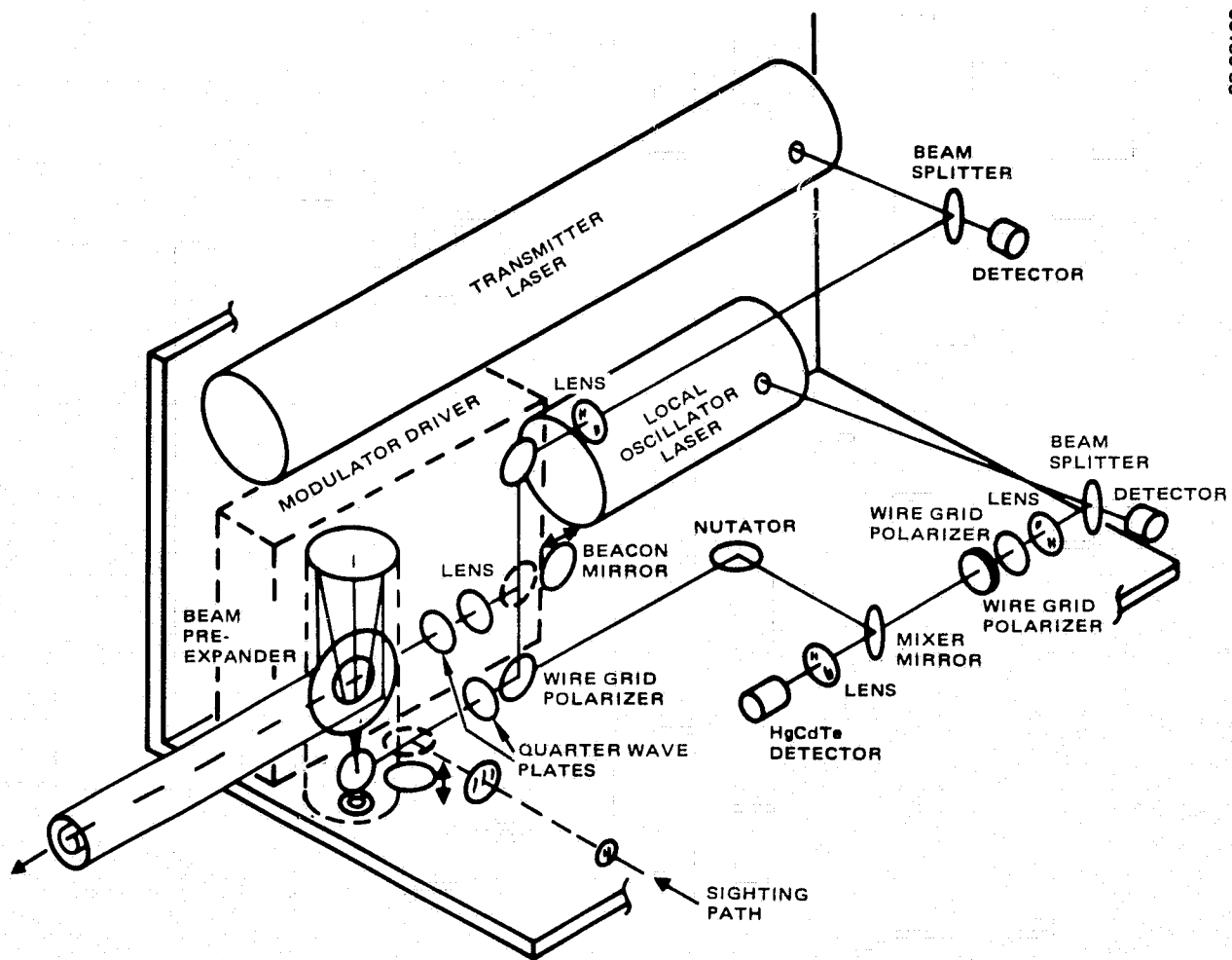
4.2 Gimbal/Structure Layout Review

4.2.12 CONCEPTUAL BASE COMPARTMENT CONTENT AND ARRANGEMENT

The only item shown in the figure that would exist in the pending brassboard model is the packaged pre-expander. Other elements would be simulated using standard laboratory equipment.

A reflective pre-expander is shown, although a refractive device has also been considered.

A single-element nutator is shown to handle the required conical scan of the received beam. It is conceivable that this device could also accommodate the point ahead requirements. A tradeoff between this and other approaches would be conducted prior to fixing the final design.



CONCEPTUAL BASE COMPARTMENT CONTENT AND ARRANGEMENT

4. Optomechanical Subsystem Design

4.2 Gimbal/Structure Layout Review

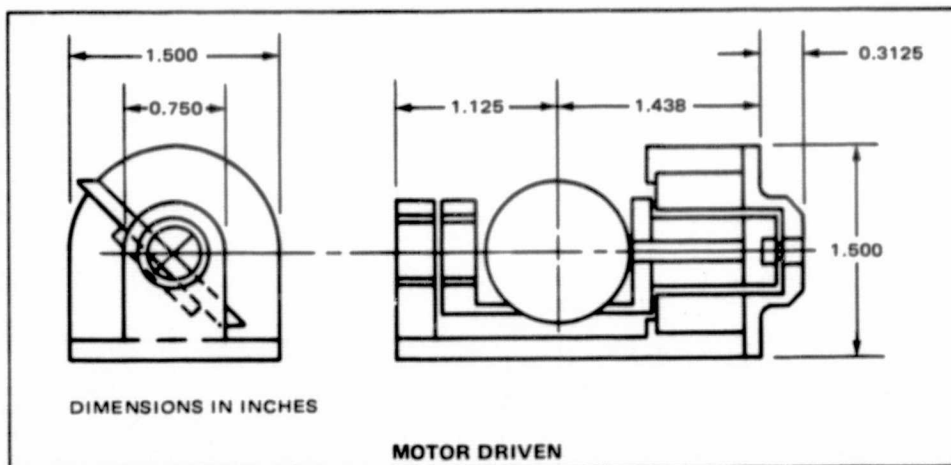
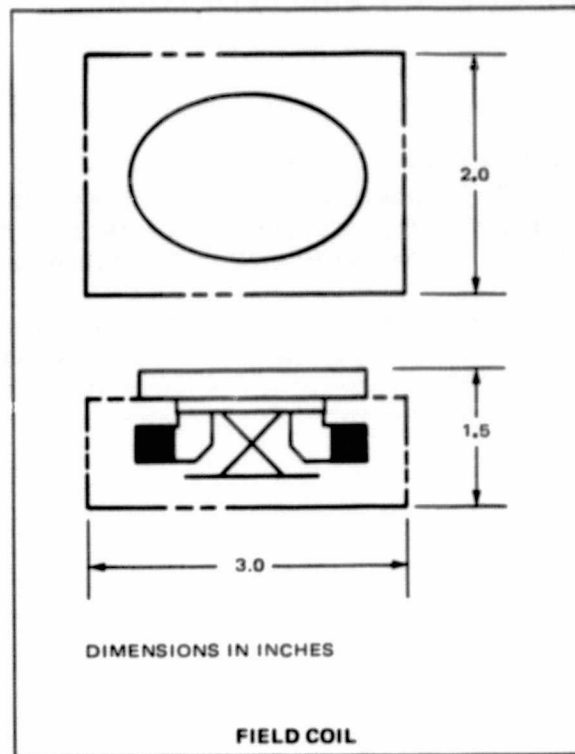
4.2.13 IMC DEVICE CONCEPTS

These two concepts for handling the larger mirrors and larger excursion angles are included to show devices that can be made to handle the ultimate system requirements. Either would have to be servo controlled to achieve the prescribed bandwidth. The field coil device would require position sensor feedback (strain gages mounted on the support flexure), while the motor driven unit would derive feedback signals from the tachometer windings in the motor.

These design concepts are only given for the purpose of component envelope definition. The field coil unit has been shown in the overall layout since it requires the larger volume.

REQUIREMENTS:

- $> \pm 1.75^\circ$ MOTION
- > 170 Hz BANDWIDTH
- POSITION READOUT CAPABILITY
- SELF CENTERING
- STANDARD ELECTRONIC OPERATION



IMC CONCEPTS

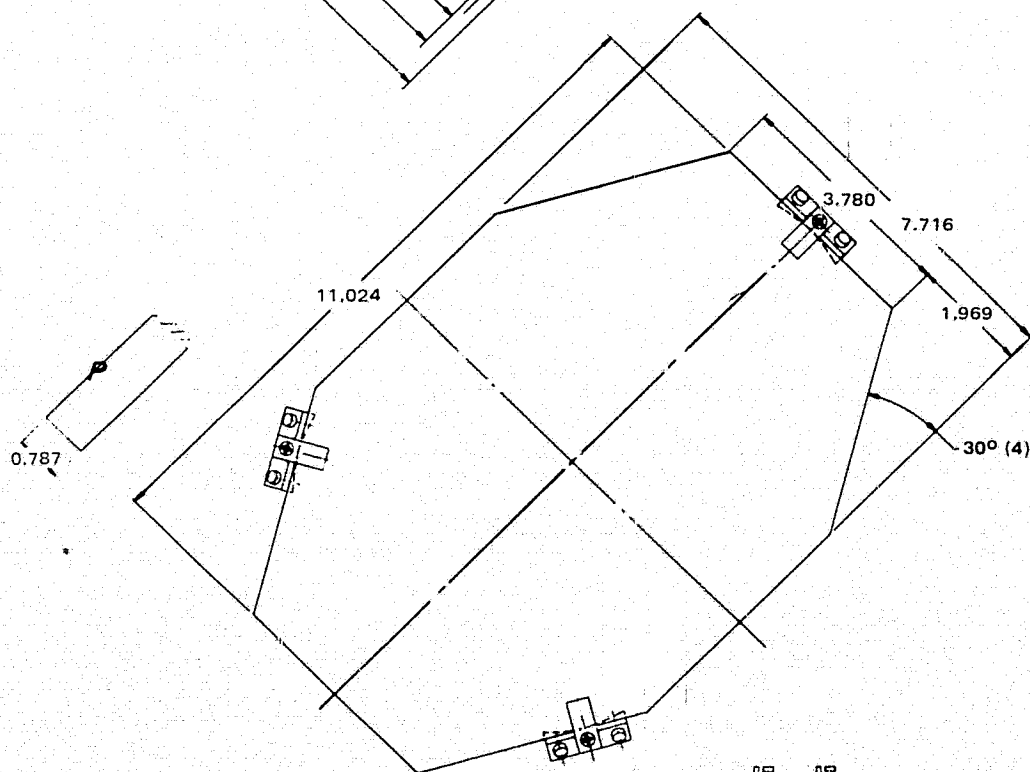
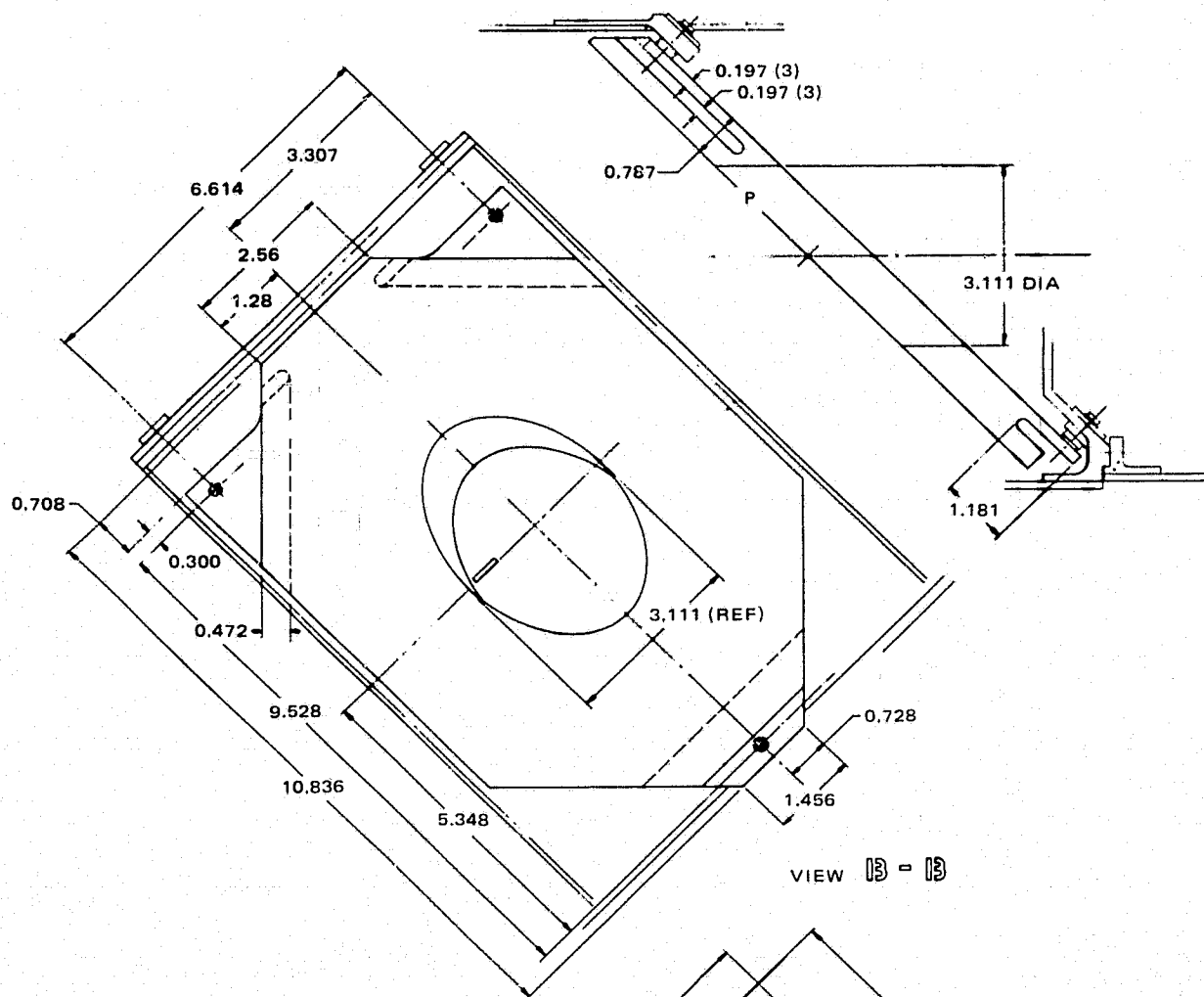
4. Optomechanical Subsystem Design

4.2 Gimbal/Structure Layout Review

4.2.14 TWO LARGE FOLDING MIRRORS

View B-B shows the outer gimbal folding mirror as it mounts in the telescope box. The mounting point arrangement allows the mirror to be firmly secured while minimizing distortion due to angular misalignments. Each of the three attach points is independently adjustable for height.

View F-F shows the much simpler mounting of the inner gimbal folding mirror. This mirror is clamped at three places to a flat surface of the inner gimbal structure. The structure itself is then adjustable for alignment at its interface with the inner gimbal motor shaft.



DIMENSIONS IN INCHES

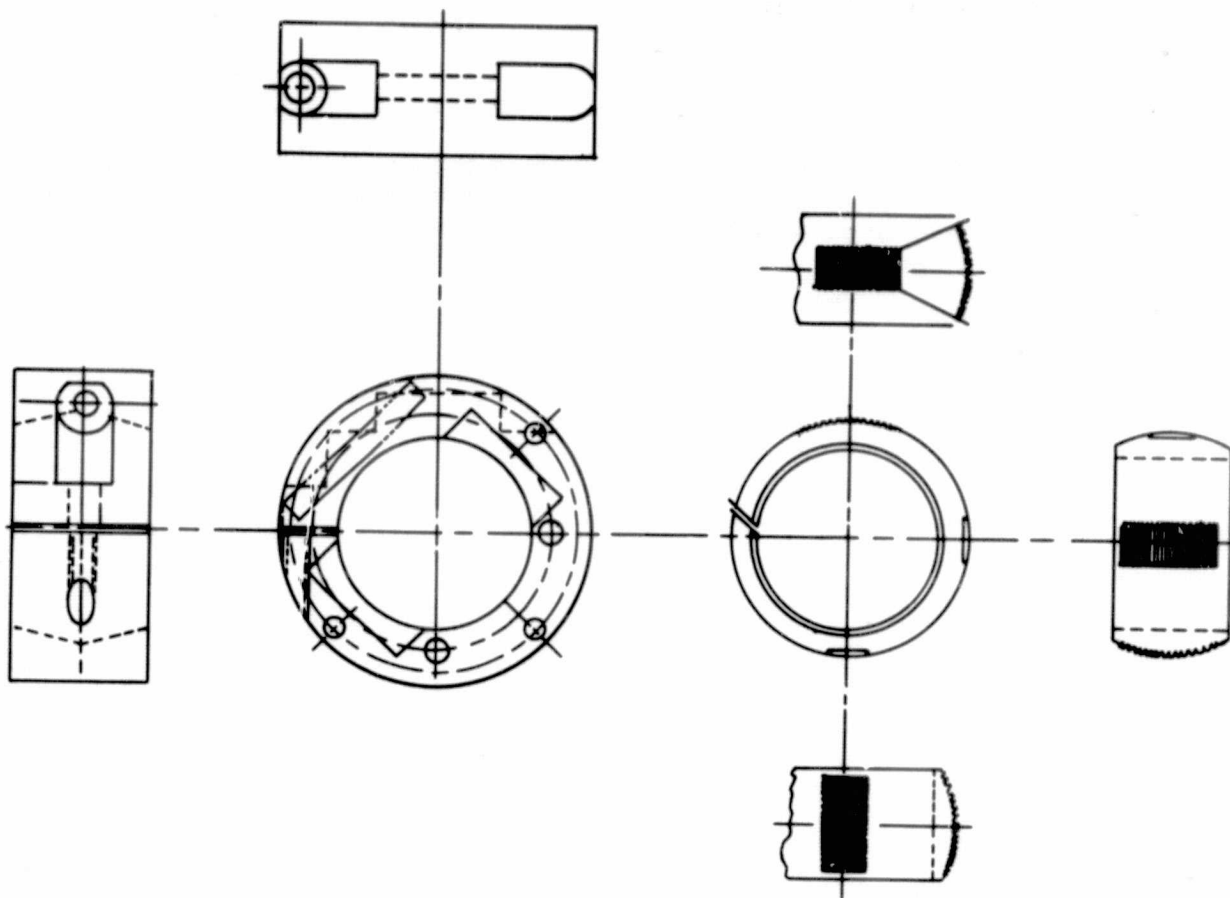
TWO LARGE FOLDING MIRRORS

4. Optomechanical Subsystem Design

4.2 Gimbal/Structure Layout Review

4.2.15 RELAY MIRROR ADJUSTMENT DEVICE

The relay mirror adjustment device is a proven design that has been used in several similar applications. Detail drawings are available. The mirror mounts to a cylinder that slips into the inner ring. This fit allows height adjustment. The outer ring mounts to the structure. With the inner ring in place, jack screws engaging the threaded portions of the inner ring provide pitch, yaw, and roll fine adjustments. The clamping screw on the outer ring then secures the entire device.



OUTER RING

INNER RING

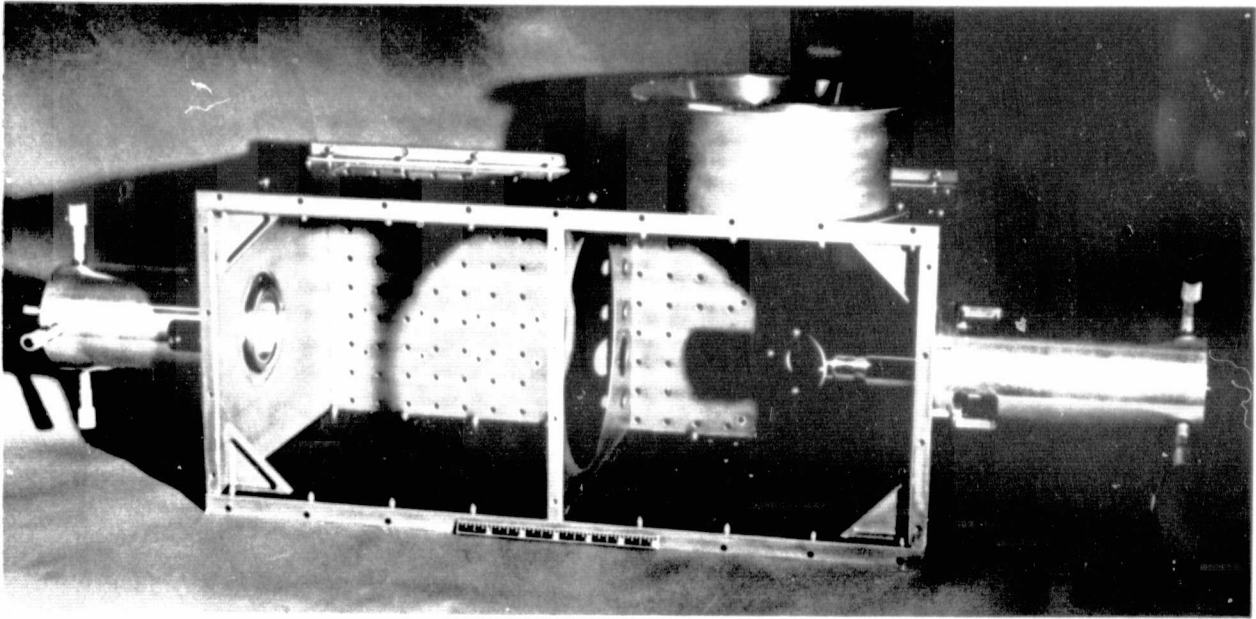
RELAY MIRROR ADJUSTMENT DEVICE

4. Optomechanical Subsystem Design

4.2 Gimbal/Structure Layout Review

4.2.16 FOCUSING ELEMENT ADJUSTMENT

The photograph of the receiver OMSS shows the focusing mirror alignment tools attached. The mirror attachments for the transmitter are the same as for the receiver OMSS. The receiver OMSS alignment tools are available and will be used for transmitter alignment.



FOCUSING ELEMENT ADJUSTMENT (PHOTO 50150-39)

4. Optomechanical Subsystem Design

4.2 Gimbal/Structure Layout Review

4.2.17 PROCURED ITEMS

The table shows items that will be procured for the brassboard model and will be suitable for eventual flight. The vendors of these components have agreed to utilize vacuum compatible materials for use in close proximity to optical surfaces. All bearing lubrication will be dry film.

PROCURED DRIVE AND CONTROL ELEMENTS

50150-407

Motor	DC direct drive brush type torque motor (Inland model T8902)
Tachometer	Kearfott model CVD 9611-003 geared 36:1 to axis for motor control (vacuum compatible materials and bearings)
Incremental encoder	Disk instrument model 862/1000-1 ALP geared 36:1 to axis for position knowledge (vacuum compatible bearings and materials)
Resolver	Kearfott model 3R-982-003 geared 1:1 to axis for detector coordinate transformation and lead angle correlation control
End of travel position indicator	Switch to be located at one end of travel each gimbal (approved Hughes part)
Gimbal bearings	KA080ARO 8 inch diameter bore, 0.250 xsect dry lubricant

4. Optomechanical Subsystem Design

4.3 Optics Design Layout Review

4.3.1 OPTICS DESIGN SUMMARY

The final configuration that was chosen for the main telescope and pre-expander optics is similar to that used for the optomechanical receiver subsystem. The tradeoff study* that reviewed the possible optical designs with respect to their applicability to the receiver subsystem is also valid for the transmitter subsystem. The Gregorian configuration has been studied in detail, and this design type offers the best design solution for a laser transmitter. Although this design effort was primarily oriented toward the system design for a transmitter, it is recognized that the transmitter and the beacon receiver will share common optics in order to reduce the overall size and weight requirements.

Central Obscuration Minimization. The output from the telescope is reflected out of a Gregorian system using a folding mirror located with its center close to the focus of the primary mirror. The folding mirror has a cutout in the center to permit light from the secondary mirror to reach the primary. This design approach minimizes the central obscuration of the output beam, in order to maximize the optical system for field gain.

Alignment Tolerance Minimization. Because of the confocal arrangement of the two positive power mirrors, the sensitivity due to the misalignments and decentrations is not as critical in other design configurations.

*Optomechanical Subsystem of a 10 Micrometer Wavelength Receiver Terminal,
Interim Test Report, September 1974, NASA Contract NAS 5-21859.

OPTICAL DESIGN REVIEW OUTLINE

FINAL OPTICAL DESIGN

- Design constraints
- Overview optical system
- Optical layout
- Beam expander design
- Pre-expander design

OPTICAL ENGINEERING

- Material
- Component fabrication
- Coating

50150-41T

4. Optomechanical Subsystem Design

4.3 Optics Design Layout Review

4.3.2 SELECTED OPTICAL DESIGN

The confocal Gregorian, with both mirrors paraboloidal, was selected as the basic design configuration for the following reasons.

Well Corrected Optical Performance. The confocal arrangement (where the focal points of the two parabolas coincide) leads to zero spherical aberration on axis and negligible coma and astigmatism for small off-axis angles.

All Reflective Design. This design allows the use of any wavelength of operation from the visible to the far infrared without the necessity of refocusing the system. (In an early design concept, the beacon was to operate at a different wavelength, 0.85 μm .)

Exit Pupil Location. The Gregorian configuration permits the exit pupil for the receiver to be located externally without the need for a separate relay system. The most favorable location for the IMCs would be at the pupil of the system; this location makes it possible for the IMCs to realign the off-axis rays with the optical axis, at the smallest optical aperture. The exit pupil was also designed as the aperture stop of the system.

Ease of Testing. This was not a design consideration, but, in general, concave mirrors are easier to manufacture and test.

SELECTED OPTICAL DESIGN

Conformal Gregorian design configuration
Paraboloidal primary and secondary mirrors

Advantages

- Well corrected optical performance
- All reflective design
- Allows location of pupil external to telescope
- Minimizes central obscuration
- Relaxes alignment tolerances
- Permits ease of testing

50150-42T

4. Optomechanical Subsystem Design

4.3 Optics Design Layout Review

4.3.3 OPTICAL DESIGN CONSTRAINTS/SPECIFICATIONS

The design constraints that were instrumental in determining the overall optical design are itemized in this topic.

Field of View, $\pm 0.5^\circ$. The central obscuration of the Gregorian telescope is essentially determined by the inside apertures in the folding mirrors. The size of these apertures is in turn dependent on the telescope acquisition field of view and the focal length of the primary mirror. The inside apertures must be sufficiently large so as not to obscure any part of the imaged field-of-view of the incoming beacon beam during acquisition. For a given field of view (1° total) and primary mirror diameter, the central obscuration can be minimized only if the focal length of the primary is minimized. This implies that the f-number of the primary must be small to minimize the power loss resulting from a central obscuration. Based on practical experience, the f-number of the primary should not fall much below f/1.5 or else the misalignment tolerances will become extremely small and thus very difficult to maintain.

Maximum IMC Dimensions. In order to achieve the necessary mirror response bandwidths with a minimum of power, it is desired that the optical element of the IMC that performs this task have as low an inertia as possible. The preferred location for this function is at, or very close to, the position where the diameter of the optical aperture is the smallest. Thus the IMCs indirectly determined the system magnification to this point.

Maximum Quarter-Wave Plate and Wide Grid Polarizer Dimensions. The sizes of available components set these sizes and contributed to the requirement of a two-stage expansion of the laser beam.

Minimum Optical Component Cost. The size of the beam expander output aperture determines the maximum achievable antenna gain for both the beacon receiver and the transmitter. However, practical considerations dictate only as large an aperture as necessary. Based on the result of a tradeoff study and fabrication cost estimates, it was concluded that an 18 cm output aperture would provide a good compromise between the overall performance and cost.

Coaxial Acquisition Beam Along the Outer Gimbal Axis. The acquisition beam must be along the outer gimbal axis since the main beam expander rotates around this axis with respect to the fixed base structure.

Maximum Energy Transfer Through the System. The gaussian beam profile of a CO₂ laser has its highest energy concentration in the center of the beam. This central portion of the beam would be lost in the presence of a central obscuration. However, once the field of view is set and the diameter of the primary is selected, the obscuration ratio is automatically determined. There are several methods for reconstituting the gaussian beam profile in order to minimize the output losses resulting from the central obscuration. The following is a brief description of the method used for the laser transmitter. Basically, this method requires the gaussian beam from the CO₂ laser to be suitably expanded so as to overfill the

aperture stop of the telescope. By broadening the beam profile, the high energy center will spread; consequently a given obscuration will block a smaller portion of the laser energy. The increase in output power is achieved by truncating the lower energy portion of the gaussian beam profile and passing more of the high power regions.

OPTICAL DESIGN CONSTRAINTS/SPECIFICATIONS

Field of view: $\pm 0.5^\circ$

Maximum IMC dimensions: 2.54 cm x 3.592 cm

Maximum quarter-wave plate and wire-grid polarizer dimensions: ≈ 20 mm

Minimize optical component cost

Coaxial acquisition beam along outer gimbal axis

Maximize energy transfer through system

50150-43T

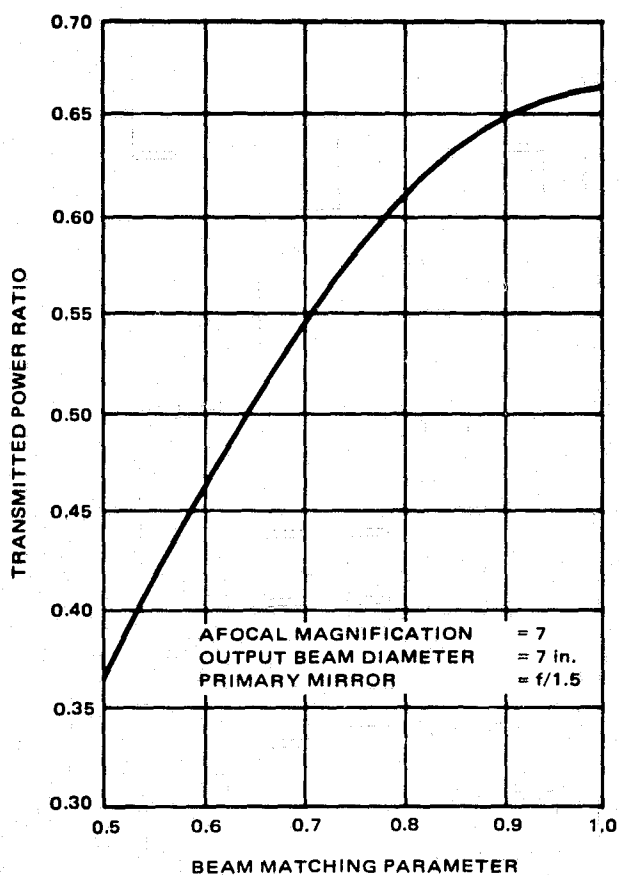
4. Optomechanical Subsystem Design

4.3 Optics Design Layout Review

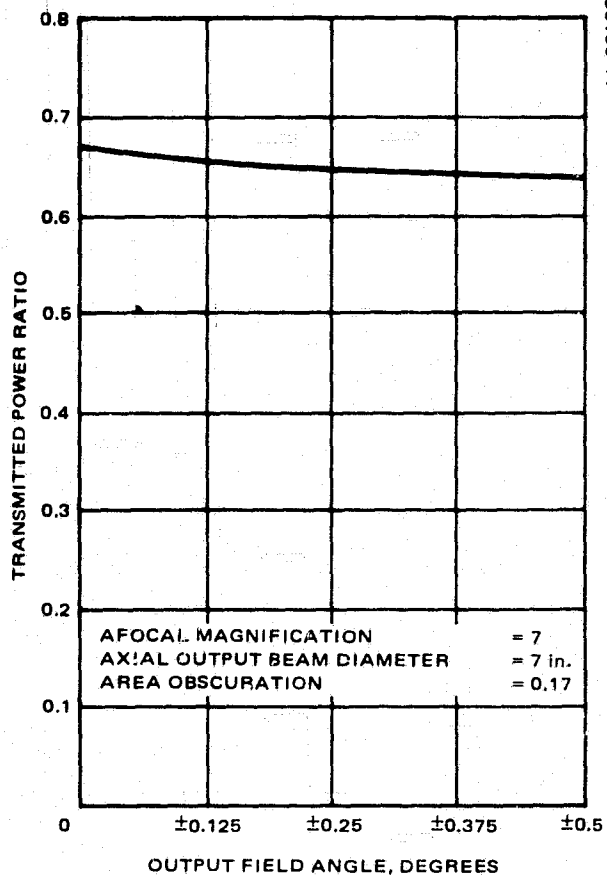
4.3.4 BEAM MATCHING AND ENERGY TRANSFER

The figure shows a plot of input to output power, "transmitted power ratio" versus a beam matching parameter (ratio of beam width to $1/e^2$ of gaussian beam), based on the method used for reconstituting the output beam profile. For this particular design the maximum power transmission is achieved when the beam matching parameter is unity, implying that the input beamwidth of the CO₂ laser should be exactly equal to the aperture stop of the system.

The second figure shows, for optimum input beam matching, the corresponding transmitted power ratio versus the output field angle. The on-axis transmitted power ratio is given as 0.668, indicating that a central area obscuration ratio of 0.17 has resulted in a power loss of 33.2 percent relative to the power of the CO₂ laser source. The corresponding power loss at the maximum field of $\pm 0.5^\circ$ is 36.2 percent. The reason for this slow falloff of energy loss is as follows: as the input beam is steered off-axis by the IMC, the central portion of the gaussian beam is no longer completely obscured by the cutout in the small folding mirror, and the energy lost by vignetting the low power region of the gaussian beam is partially made up by passing more of the high power, central region.



TRANSMITTED POWER RATIO VERSUS BEAM MATCHING PARAMETER



TRANSMITTED POWER RATIO VERSUS OUTPUT FIELD ANGLE

BEAM MATCHING AND ENERGY TRANSFER

50150-44

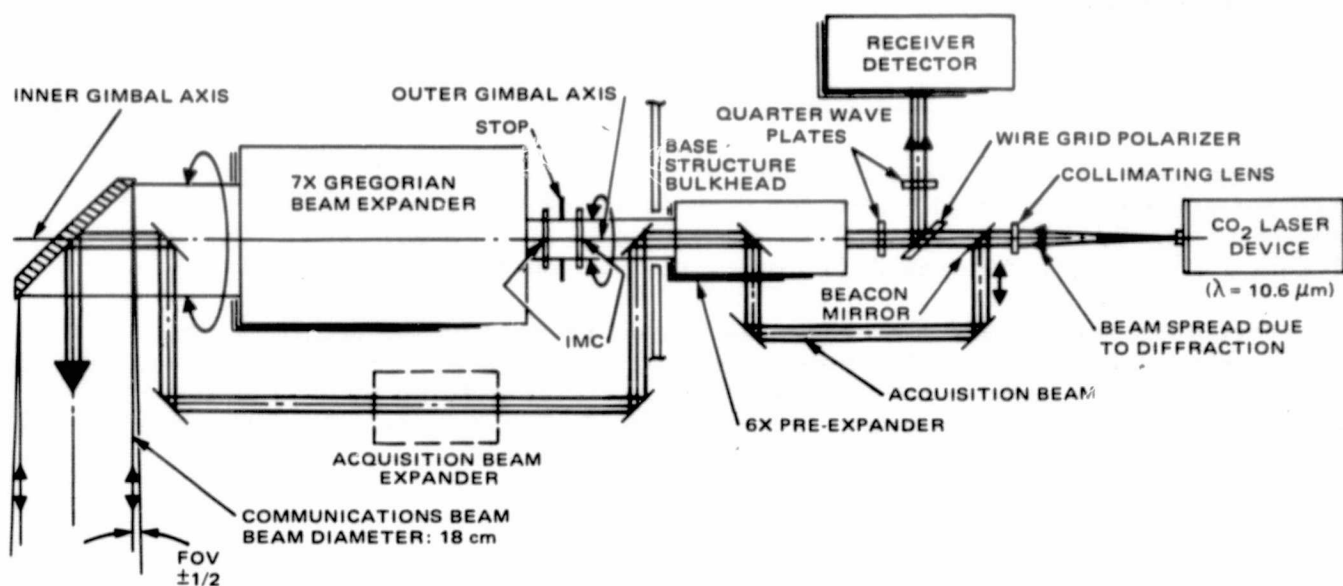
4. Optomechanical Subsystem Design

4.3 Optics Design Layout Review

4.3.5 OPTICAL SCHEMATIC OVERVIEW

The figure is an optical schematic that shows the basic subsystems in the transmitter/receiver optical design. The linearly polarized, modulated output beam from the CO₂ laser device has a beam waist diameter of 1 mm at the $1/e^2$ point. The beam is allowed to diverge to 4.4 mm where it is collimated prior to entering the 6X pre-expander. This collimated beam is then transmitted through a beamsplitter and a quarter-wave plate. The beamsplitter is a wire-grid polarizer and, together with the quarter-wave plate, converts the transmitted beam into a right-handed, circularly polarized beam. The beam is directed through the pre-expander by relay mirrors to the IMC package.

The schematic also shows the path for the initial acquisition beam. This beam is extracted by the movable beam mirror and injected coaxially with the communication beam along the outer-gimbal axis. The diameter of this acquisition beam is sized so that the beam angular diffraction is the desired field of view for the initial acquisition system.



OPTICAL SCHEMATIC OVERVIEW

4. Optomechanical Subsystem Design

4.3 Optics Design Layout Review

4.3.6 OPTICAL LAYOUT

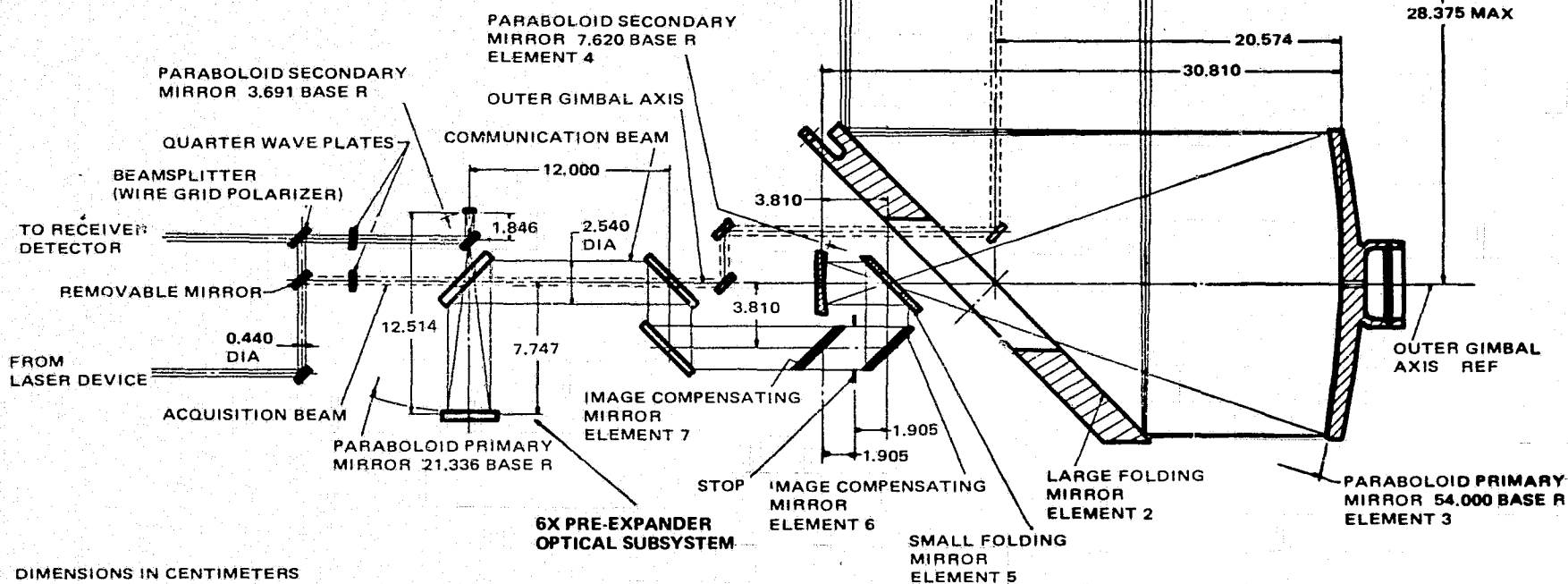
The transmitted 10.6 μm laser beam undergoes two stages of beam expansion. The first stage uses a 6X all reflector pre-expander which magnifies the beam diameter from 0.44 to 2.54 cm. The second stage is a 7X all reflective afocal telescope which magnifies the 2.54 cm beam to an output beam diameter of 18 cm.

These two beam expanders also serve as the receiving and demagnifier optics for the incoming laser beacon. Beamsplitting is performed for the incoming beacon beam behind the two afocal telescopes. The receiver optics, which are not shown, then image the beacon beam energy onto a photodiode detector using an optical condenser.

LIMIT RAY DATA	
SURFACE	LIMIT RAY
IMC MIRROR ELEM 7	1.796°
STOP	1.270
IMC MIRROR ELEM 6	1.796°
SMALL FOLDING MIRROR ELEM 5	2.152°
SECONDARY MIRROR ELEM 4	1.652
PRIMARY MIRROR ELEM 3	8.999
LARGE FOLDING MIRROR ELEM 2	12.861°
POINTING MIRROR	13.451°

*MEASURED ALONG MIRROR SURFACE

OPTICAL CHARACTERISTICS	
MAGNIFICATION	7.0866
F - NUMBER PRIMARY	1.5
F - NUMBER SECONDARY	1.15
FIELD OF VIEW	$\pm 1/2^\circ$
DIAMETER OBSCURATION RATIO	0.417
OUTPUT BEAM DIAMETER	18 cm (7.0866 in.)



OPTICAL LAYOUT

4. Optomechanical Subsystem Design

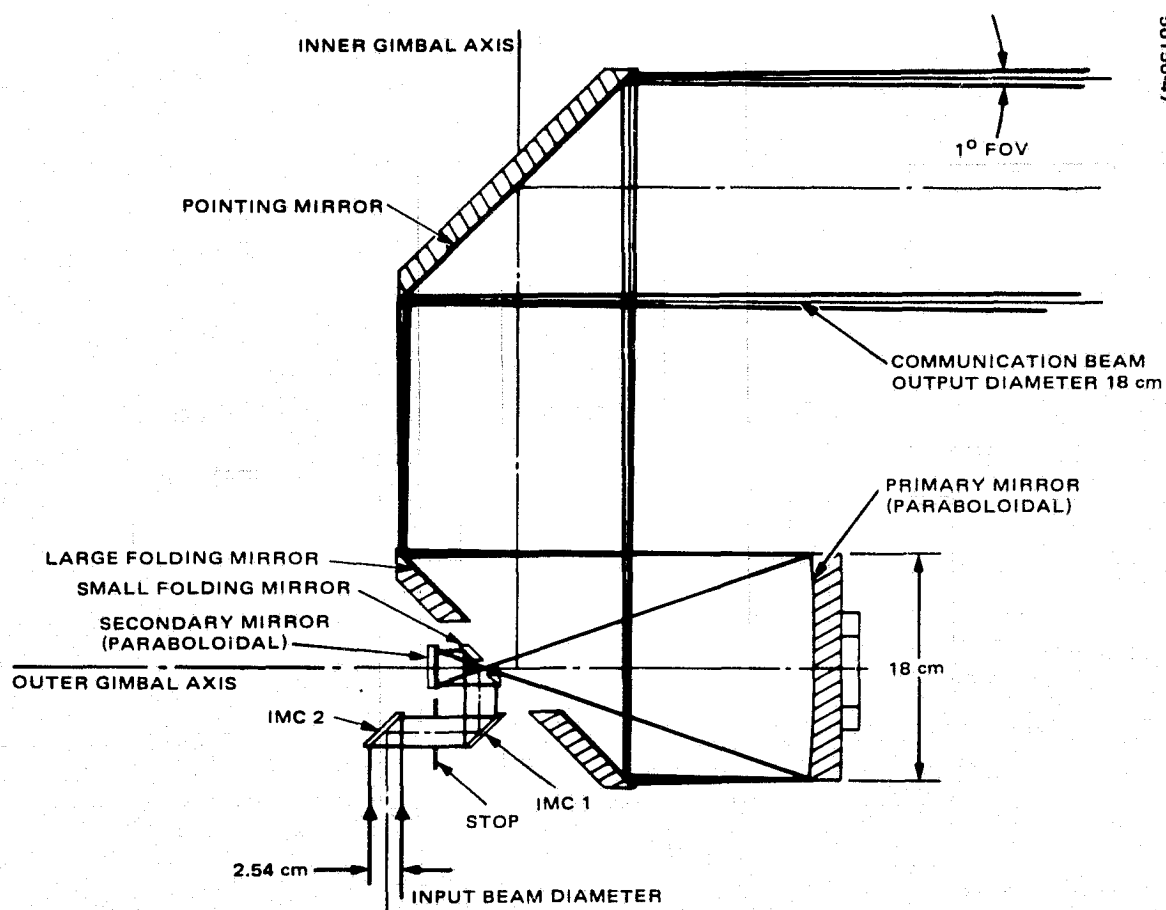
4.3 Optics Design Layout Review

4.3.7 7X GREGORIAN BEAM EXPANDER

The IMC mirrors direct the transmitted laser beam to a small folding mirror with a central cutout into the 7X beam expander. The beam expander consists of two confocal paraboloids with a common focus located at the center of the small folding mirror. The f-numbers of the primary and secondary paraboloidal mirrors are 1.5 and 1.15, respectively. Situated between the small folding mirror and the primary mirror is a large 45° folding mirror. The central cutout in the large folding mirror is matched to that of the small folding mirror. The final output beam is directed by the pointing mirror to the distant receiver.

Two-axis pointing capability is achieved by rotating the pointing mirror about the inner gimbal axis and the main telescope beam expander about the outer gimbal axis. The outer gimbal axis also coincides with the optical axis of the telescope.

The stop of the system and the entrance pupil are both located at the plane midpoint between the two IMC mirrors. The diameter of the stop is 2.54 cm. The central area obscuration ratio of the system is 0.17, corresponding to a diameter obscuration ratio of 0.417. The limiting ray heights at the key elements are shown on the optical layout. When the system is used in the receiving mode for initial acquisition, the incoming beam, within the acquisition field of view of $\pm 0.5^\circ$, is directed by the pointing mirror into the telescope via the large folding mirror. The beam emerging from the IMC package has been demagnified by 7X. The polarization state of this beam is left-handed, circularly polarized, the reverse of the outgoing transmitted beam.



7X GREGORIAN BEAM EXPANDER

4. Optomechanical Subsystem Design
4.3 Optics Design Layout Review

4.3.8 OPTICAL CHARACTERISTICS OF 7X GREGORIAN BEAM EXPANDER

This table summarizes the important optical characteristics of the main telescope beam expander.

7X GREGORIAN BEAM EXPANDER OPTICAL CHARACTERISTICS

50150-48T

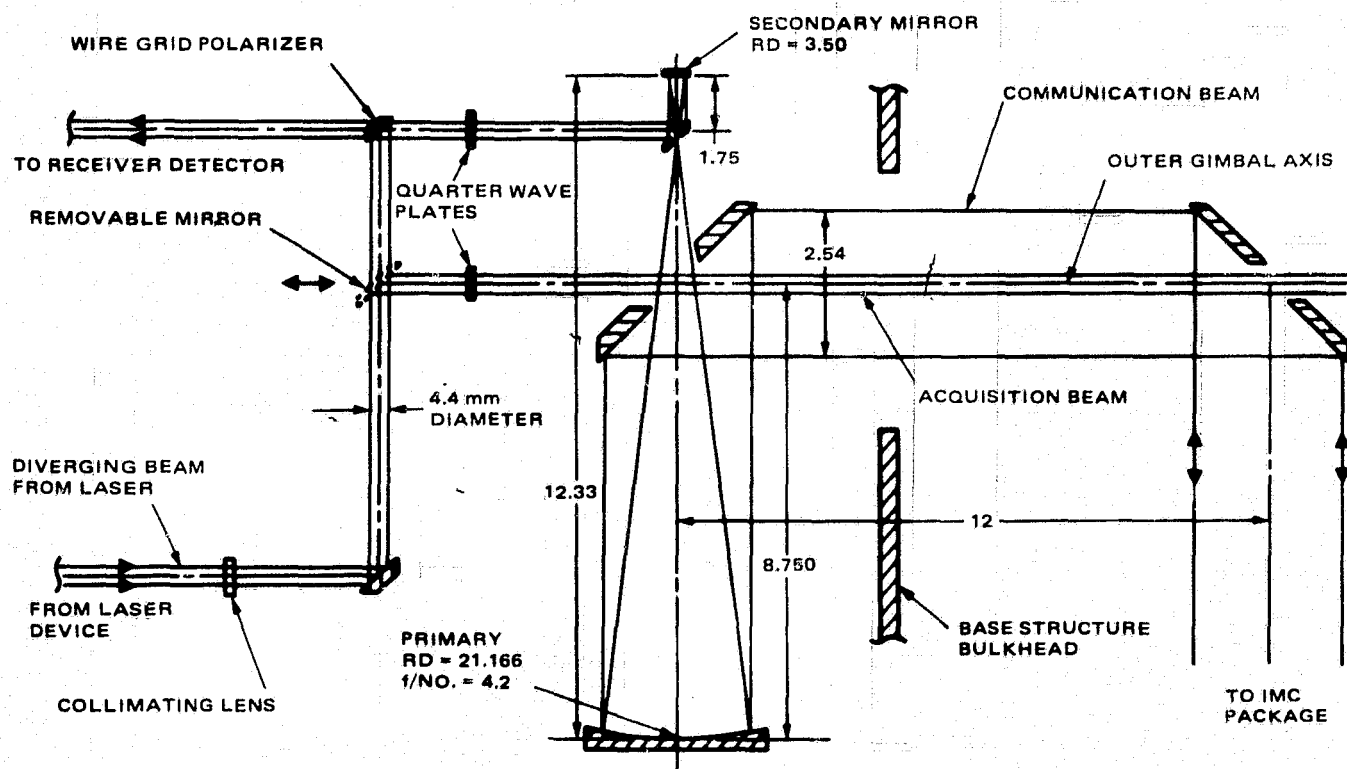
<u>Parameter</u>	<u>Value</u>
Design configuration	Folded afocal Gregorian system with confocal paraboloidal primary and secondary mirrors
Diameter of primary	18 cm
Diameter of secondary	3.305 cm
Diameter of on-axis output beam	18 cm
f-number of primary	1.5
f-number of secondary	1.15
Afocal magnification	7.0866
Output field of view	$\pm 0.5^\circ$
Diameter obscuration ratio	0.417
Spectral region	10.6 μm
Diameter of stop	2.54 cm

4. Optomechanical Subsystem Design

4.3 Optics Design Layout Review

4.3.9 6X GREGORIAN PRE-EXPANDER

The figure is a sketch of the basic components for the all reflective pre-expander. The incoming laser beam is allowed to diverge to 0.44 cm so as to overfill the 0.42 cm diameter secondary for maximum beam matching and energy transfer. The 0.42 cm beam is then magnified 6.046 times to provide an output beam diameter of 2.54 cm. The 2.54 cm beam is the input to the main telescope optics. The physical dimensions of the pre-expander have been designed so as to accommodate the incoming beacon beam without additional vignetting or obscuration.



DIMENSION IN CENTIMETERS
UNLESS OTHERWISE NOTED

6X GREGORIAN PRE-EXPANDER

4. Optomechanical Subsystem Design

4.3 Optics Design Layout Review

4.3.10 OPTICAL CHARACTERISTICS OF 6X GREGORIAN PRE-EXPANDER

The table summarizes the important optical characteristics of the 6X pre-expander.

6X GREGORIAN PRE-EXPANDER OPTICAL CHARACTERISTICS

Design configuration

Folded afocal Gregorian system with confocal
paraboloidal primary and secondary mirrors

Diameter of primary

2.54 cm

Diameter of secondary

0.42 cm

f-number of primary

4.17

f-number of secondary

4.17

Afocal magnification

6.046

Diameter obscuration ratio

0.173

50150-501

4. Optomechanical Subsystem Design

4.3 Optics Design Layout Review

4.3.11 OPTICAL LAYOUT SHOWING LOCATIONS OF ELEMENTS 1 THROUGH 13

The figure indicates the location of optical elements 1 through 13 for which drawings will be released and components will be fabricated during the hardware phase of the LDRL contract.

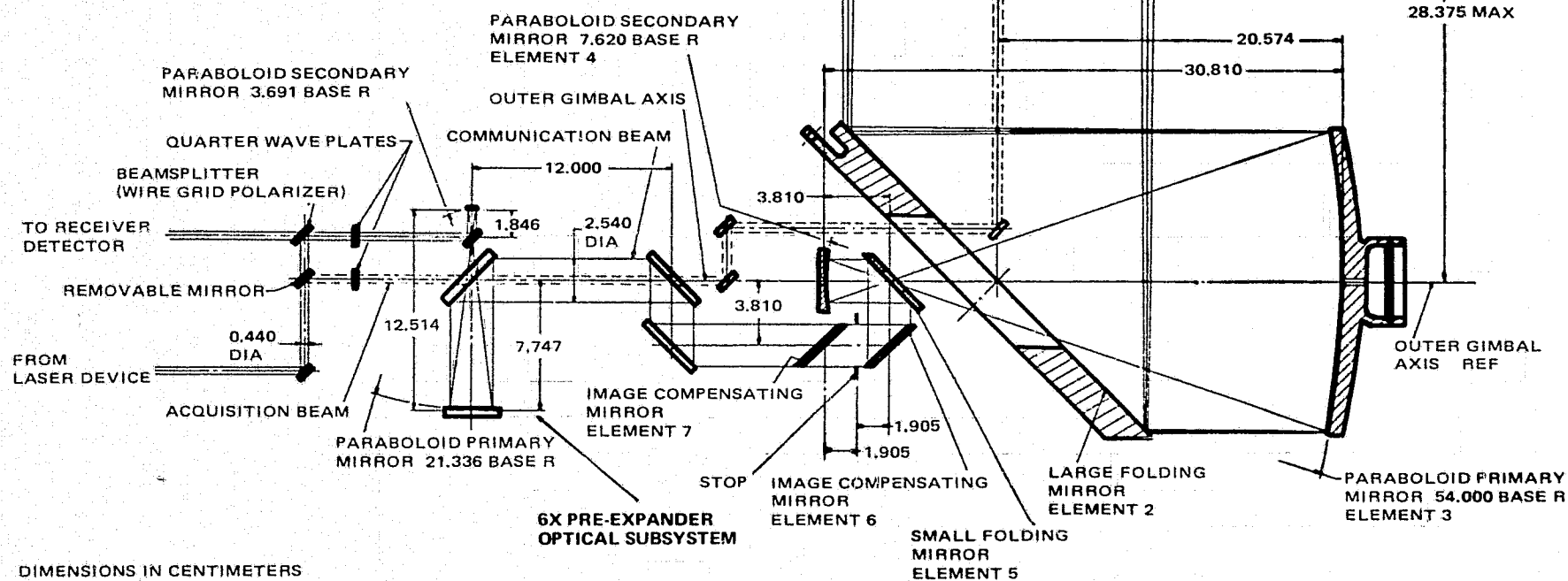
Present direction is to fabricate all 13 reflective optical elements from beryllium plated with nickel (0.004 to 0.006 inch) and build the inner and outer gimbal housings in as near a flight configuration as possible within the budget constraints. The main laser housing compartment has the lowest priority and will require more extensive refurbishment to update it to a flight configuration.

In the main laser housing is the laser pre-expander, elements 10 through 13. If it proves to be cost effective, these elements will also be fabricated from electroless nickel plated beryllium. It is presently thought that enough excess beryllium material will be available from the fabrication of mirrors 1 through 13 to make this cost effective. The pre-expander will be mounted and aligned in a cylindrical lens housing.

LIMIT RAY DATA	
SURFACE	LIMIT RAY
IMC MIRROR ELEM 7	1.796°
STOP	1.270
IMC MIRROR ELEM 6	1.796°
SMALL FOLDING MIRROR ELEM 5	2.152°
SECONDARY MIRROR ELEM 4	1.652
PRIMARY MIRROR ELEM 3	8.999
LARGE FOLDING MIRROR ELEM 2	12.861°
POINTING MIRROR	13.451°

* MEASURED ALONG MIRROR SURFACE

OPTICAL CHARACTERISTICS	
MAGNIFICATION	7.0866
F - NUMBER PRIMARY	1.5
F - NUMBER SECONDARY	1.15
FIELD OF VIEW	$\pm 1/2^\circ$
DIAMETER OBSCURATION RATIO	0.417
OUTPUT BEAM DIAMETER	18 cm (7.0866 in.)



DIMENSIONS IN CENTIMETERS

OPTICAL LAYOUT

4. Optomechanical Subsystem Design

4.3 Optics Design Layout Review

4.3.12 PRELIMINARY BERYLLIUM COMPONENT DRAWINGS

At present the 13 preliminary mirror drawings shown, mirror elements 1 through 13, have been submitted to optical fabrication vendors for their consideration in fabrication and coating. The elements will be designed, fabricated, and coated in the construction phase of this program.

The ratio of 14 to 1 for a length to thickness ratio has been established for all elements except for the smaller components within the pre-expander. These will be somewhat thicker for ease in handling and cleaning. Mechanical interfaces have been established for most of the mirrors using former designs and providing integrated alignment features where practical.

In general the mirrors, except for the pre-expander, will have surface accuracy of 1 wavelength spherical power and irregularity at 6328 \AA with elements in the pre-expander requiring a tighter figure tolerance. The lateral alignment tolerance has been set at $\pm 0.5 \text{ mm}$ for all except the pre-expander mirrors.

PRELIMINARY BERYLLIUM COMPONENTS

Element	Name	Approximate Size, cm	Approximate thickness, cm
1	Flat pointing mirror - flat	28 x 19.5	2
2	Flat folding mirror	28 x 19.5	2
3	Primary mirror paraboloid	18	14 to 1
4	Secondary mirror paraboloid	4	14 to 1
5	Flat, small folding mirror	4.5 x 3	14 to 1
6 and 7	IMC flats (two each)	2.54 x 3.59	14 to 1
8 and 9	Flat folding mirror (two each)	2.54 x 3.59	14 to 1
10	Pre-expander large folding mirror	3.59 x 2.54	12 to 1
11	Pre-expander paraboloid primary	2.75	12 to 1
12	Pre-expander paraboloid secondary	6	10 to 1
13	Pre-expander small folding mirror	0.622 x 0.44	10 to 1

50150-52T

4.3 Optics Design Layout Review

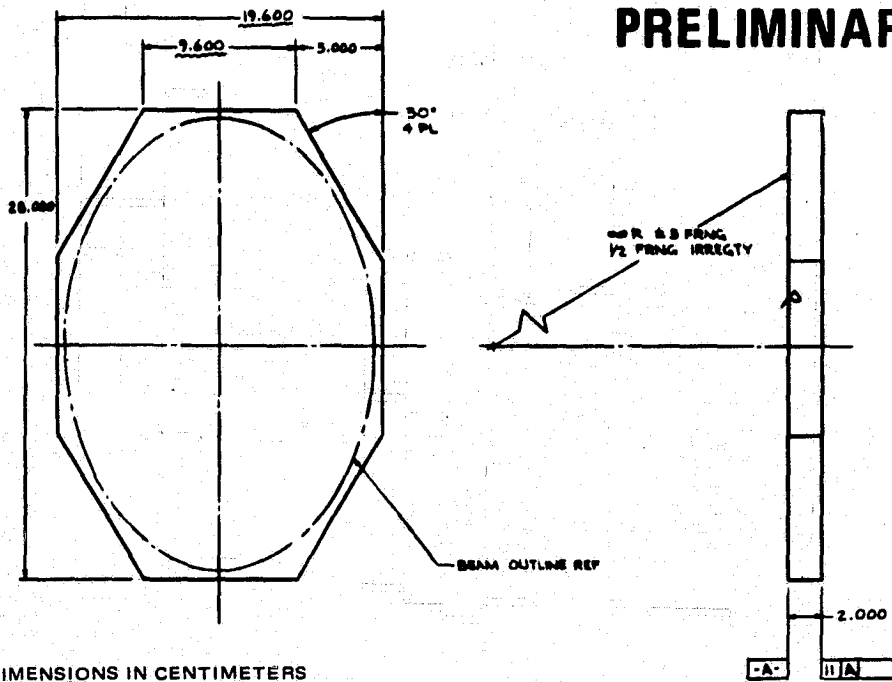
4.3.12 Preliminary Beryllium Component Drawings

4.3.12.1 ELEMENT 1: FLAT POINTING MIRROR

The flat pointing mirror will be octagonal in shape to minimize material and machining costs. The component fabrication notes that will eventually be added to the drawings have evolved through extensive experience at Hughes in space optics, including the design and fabrication of beryllium mirrors at cryogenic temperatures.

PRELIMINARY

50150-53



ELEMENT 1: FLAT POINTING MIRROR

4.3 Optics Design Layout Review

4.3.12 Preliminary Beryllium Component Drawings

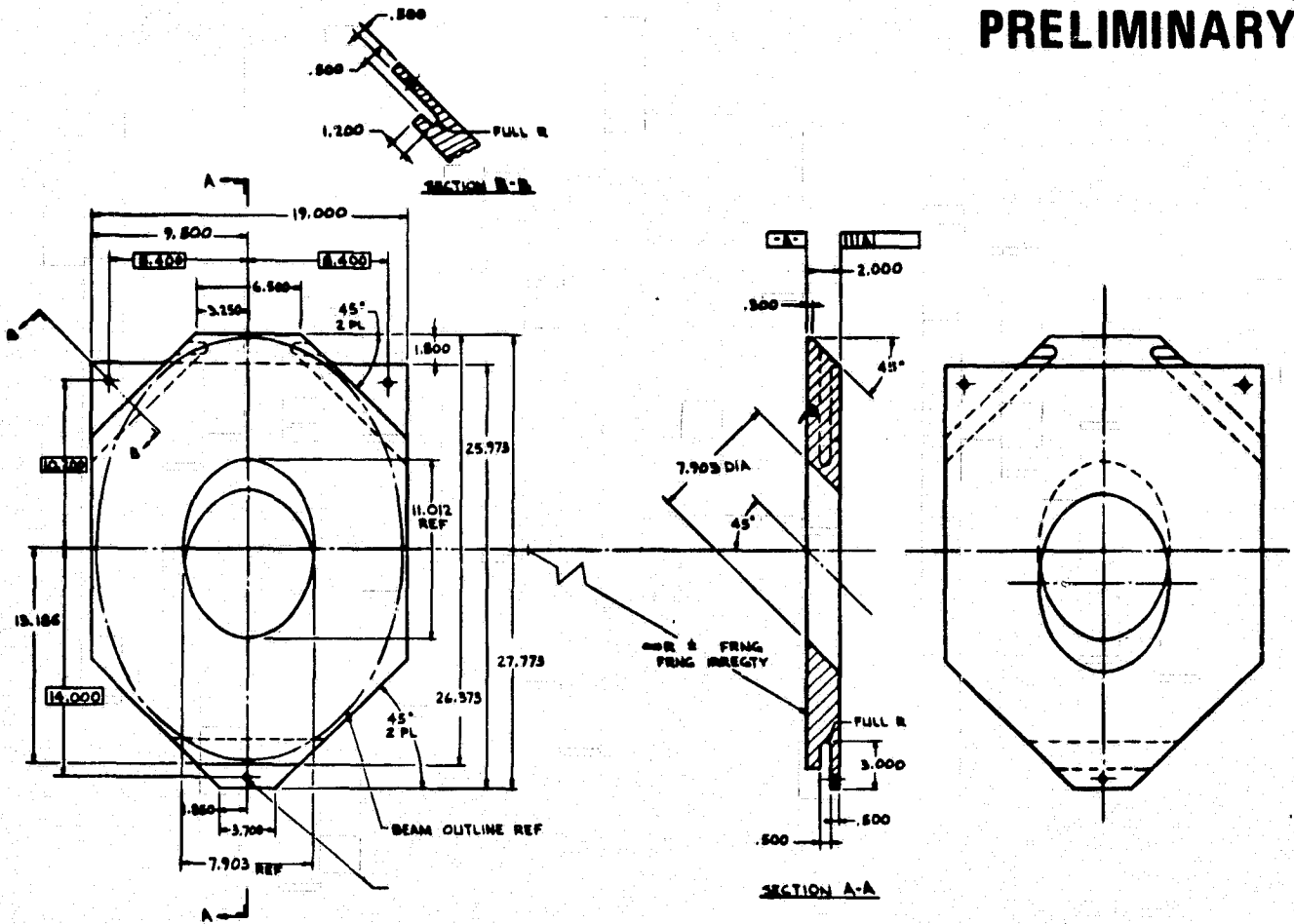
4.3.12.2 ELEMENT 2: FLAT FOLDING MIRROR

Of particular importance in the flat folding mirror are the tabs that have been designed into the mirrors to isolate the stress induced by adjusting screws used for mounting and alignment purposes.

Adjusting Screw Assembly. A schematic drawing of the adjusting screw assembly is shown in the figure. The spherical washers, adjusting screw, and mirror tab surface are all seated on optically smooth surfaces. An alignment tool is available which contains a concentric pair of screwdrivers. The procedure is to first set up the correct mirror alignment with the adjusting screw and then lock the assembly by tightening the lock screw which expands the adjusting screw at the top. The spherical washers when seated properly prevent mirror parts from bending since most of the bending occurs in the lock screw itself.

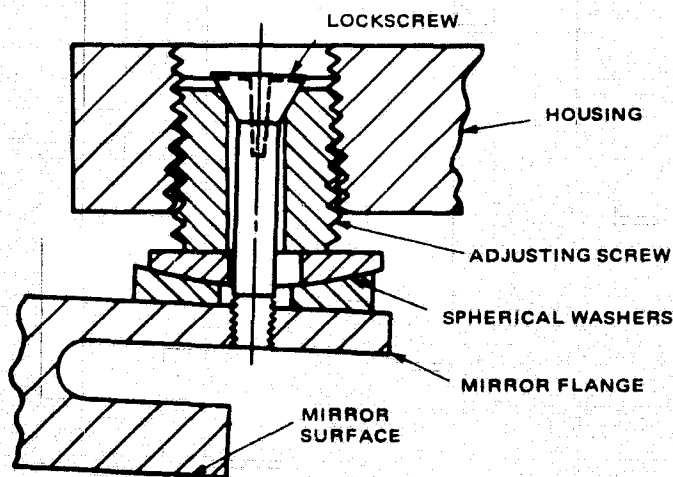
PRELIMINARY

50150-54



DIMENSIONS IN CENTIMETERS

ELEMENT 2: FLAT FOLDING MIRROR



50150-55

ADJUSTING SCREW ASSEMBLY

4.3 Optics Design Layout Review

4.3.12 Preliminary Beryllium Component Drawings

4.3.12.3 ELEMENT 3: PRIMARY MIRROR

The primary mirror contains a mounting flange shown in more complete detail with the mating parts in the optomechanical design subsystem section. The mounting and alignment flange is integral with the beryllium structure and uses the exact design used in the OMSS receiver. By utilizing this design, Hughes is able to use the present OMSS receiver alignment tool. Dimensional alignment freedom (i. e., lateral, angular, and axial) is provided by this design. A small central hole is also provided for alignment.

50150-56



ELEMENT 3: PRIMARY MIRROR

4.3 Optics Design Layout Review

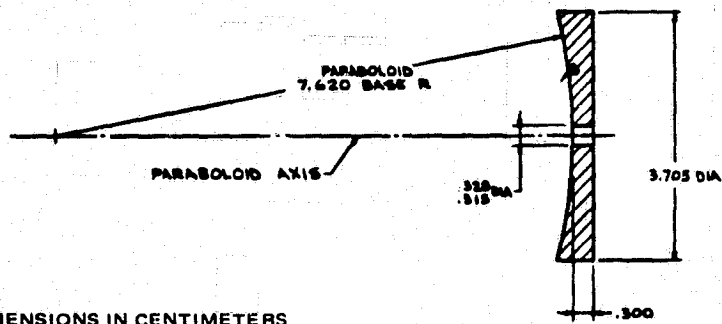
4.3.12 Preliminary Beryllium Component Drawings

4.3.12.4 ELEMENT 4: SECONDARY MIRROR

The secondary mirror may also include an integral base flange as is designed into the primary mirror, Element 3, if this proves to be cost effective.

PRELIMINARY

50150-57



DIMENSIONS IN CENTIMETERS

ELEMENT 4: SECONDARY MIRROR

4.3 Optics Design Layout Review

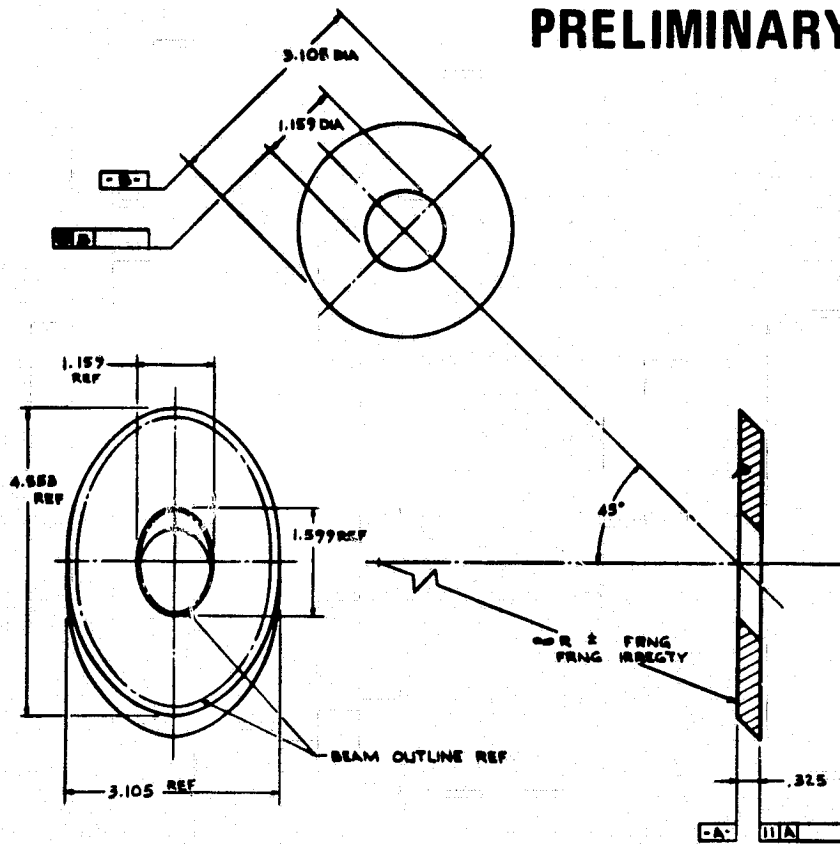
4.3.12 Preliminary Beryllium Component Drawings

4.3.12.5 ELEMENT 5: SMALL FOLDING MIRROR

The obscuration ratio of 0.417 is established with the small folding mirror. A lateral alignment tolerance of ± 0.5 mm in the central hole has been included in design.

PRELIMINARY

50150-58



DIMENSIONS IN CENTIMETERS

ELEMENT 5: SMALL FOLDING MIRROR

4.3 Optics Design Layout Review

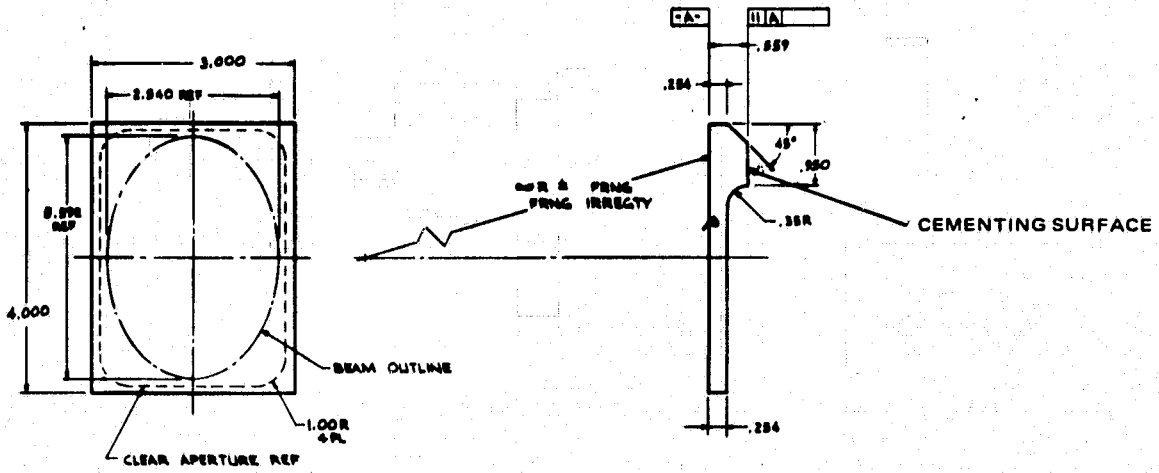
4.3.12 Preliminary Beryllium Component Drawings

4.3.12.6 ELEMENTS 6 AND 7: TWO FLAT IMC MIRRORS

The two flat IMC mirrors are designed to be cemented to the IMC mechanical interface as indicated. GTE PBM-8G devices supplied by GTE will likely be used in the proposed brassboard model. This will be done in mockup volumes representing the final IMCs.

PRELIMINARY

50150-59



DIMENSIONS IN CENTIMETERS

ELEMENTS 6 AND 7: TWO FLAT IMC MIRRORS

4.3 Optics Design Layout Review

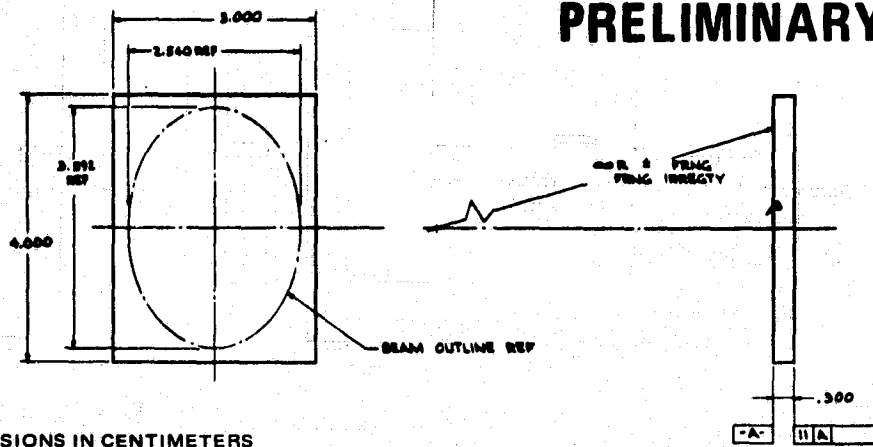
4.3.12 Preliminary Beryllium Component Drawings

4.3.12.7 ELEMENTS 8 AND 9: TWO FLAT FOLDING MIRRORS

The flat folding mirrors direct the laser beam coaxials with the outer gimbal axis. In the final design, one of these mirrors will require a central hole to accommodate the acquisition beam. This hole would be sized such that the obscuration ratio is still established by element 5.

PRELIMINARY

50150-60



DIMENSIONS IN CENTIMETERS

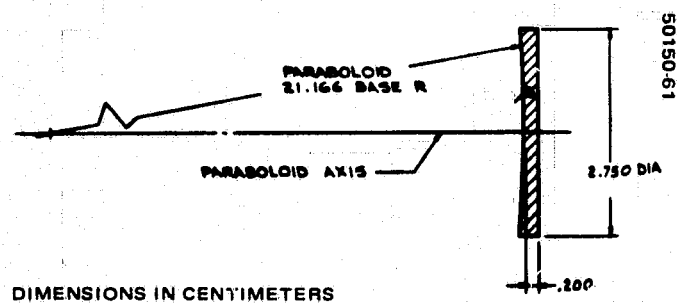
ELEMENTS 8 AND 9: TWO FLAT FOLDING MIRRORS

4.3 Optics Design Layout Review

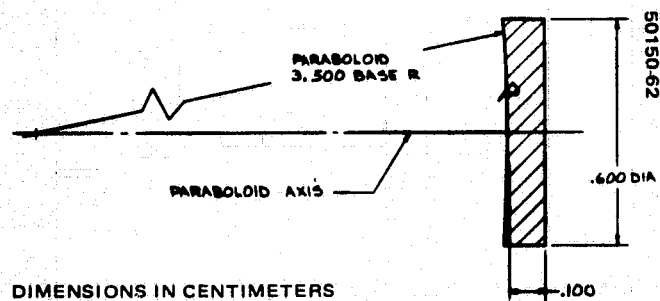
4.3.12 Preliminary Beryllium Component Drawings

4.3.12.8 ELEMENTS 10 THROUGH 13: PRE-EXPANDER ASSEMBLY MIRRORS

The four pre-expander assembly mirrors are shown in the four preliminary drawings. It is anticipated that these four mirrors also will be fabricated from nickel plated beryllium. These mirrors will be assembled and prealigned in a cylindrical lens housing.



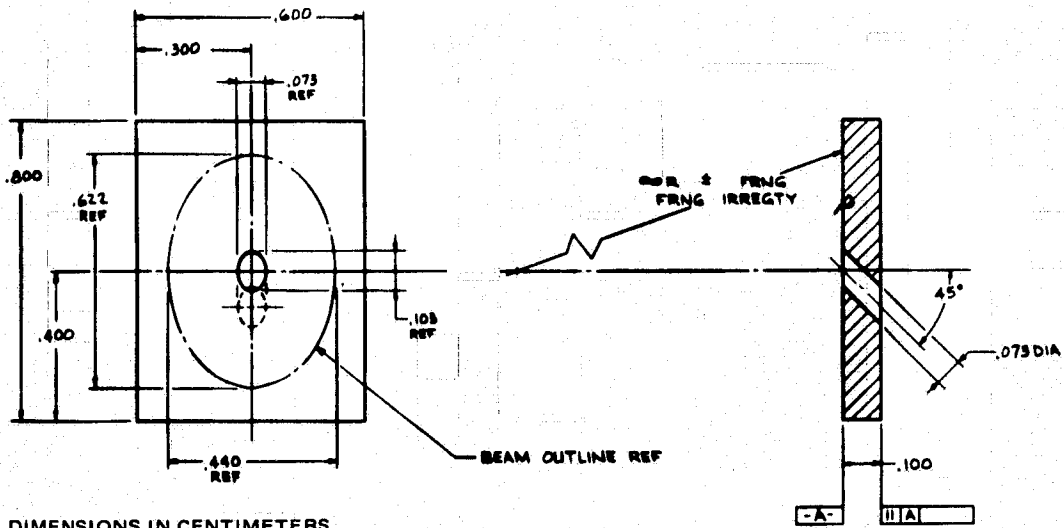
ELEMENT 10: PRIMARY PRE-EXPANDER MIRROR



ELEMENT 11: SECONDARY PRE-EXPANDER MIRROR

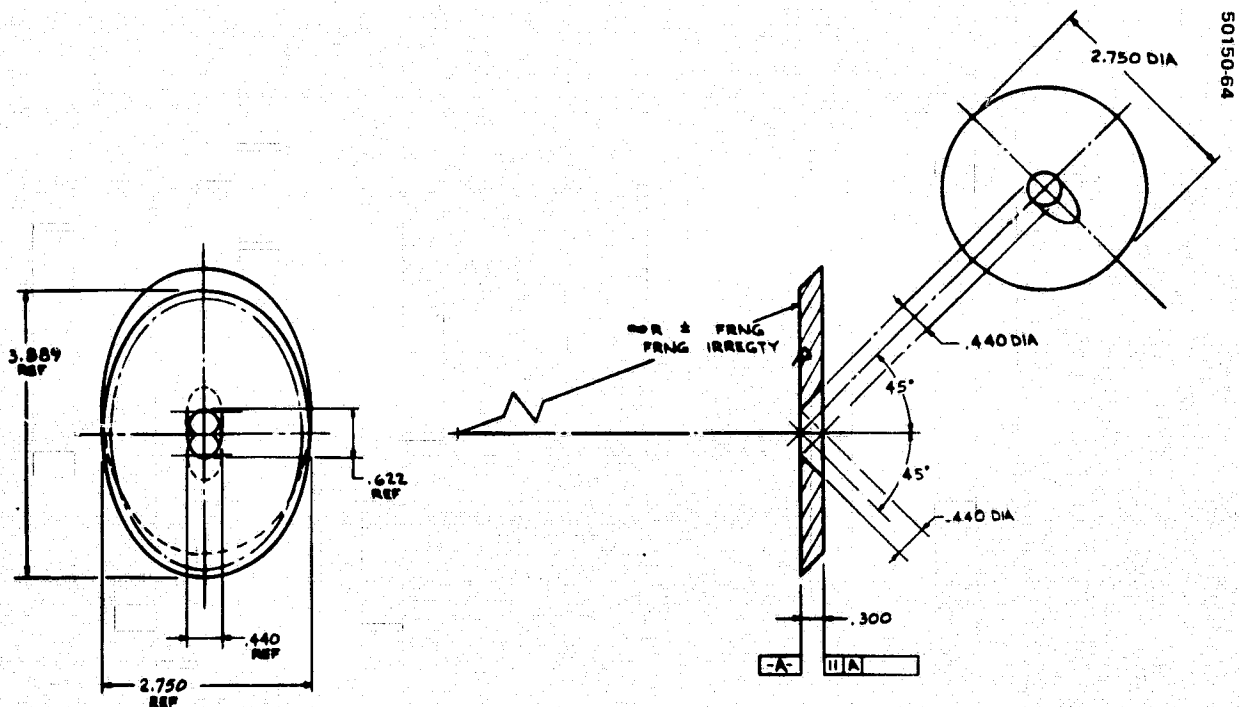
PRELIMINARY

50150-63



DIMENSIONS IN CENTIMETERS

ELEMENT 12: SMALL FOLDING PRE-EXPANDER MIRROR



DIMENSIONS IN CENTIMETERS

ELEMENT 13: LARGE FOLDING PRE-EXPANDER MIRROR

4. Optomechanical Subsystem Design

4.3 Optics Design Layout Review

4.3.13 MATERIAL

The choice of nickel plated beryllium for mirror material is based on the design objective of constructing a brassboard in a flight hardware configuration. HP 81 or I70A beryllium is preferred due to its low oxide content and because it is highly isotropic. The 0.004 to 0.006 inch electroless nickel plating enables figuring to excellent surface quality and accuracy. The low overall weight, due to the high stiffness ratio of beryllium and its low density, is both highly desirable in a Shuttle launch and orbital environment. The low coefficient of thermal expansion (low magnitude of thermal distortion) will enable reasonable environmental temperature gradients with dimensional stability, a paramount consideration in mirror design.

MATERIAL

Nickel plated beryllium

HP 81 or 170 A

Flight hardware simulation

Light weight

Low coefficient of thermal expansion

Easily plated with electroless nickel

50150-65T

5. OPTOMECHANICAL SUBSYSTEM AND 10 MICROMETER RECEIVER MEASUREMENTS

The measurement program will integrate the waveguide local oscillator, the servo drive electronics, and the AIL receiver with its doppler tracking electronics into the optomechanical subsystem. This will provide a complete optical heterodyne receiver which will then be tested and evaluated to determine its performance characteristics. The components to be integrated were developed under contracts NAS 5-21859, NAS 5-23119, NAS 5-23183, and NAS 5-23211.

Receiver Integration and Packaging. The three major units that form the 10.6 micrometer receiver terminal are shown in the block diagram. The hardware is separated into three portions. The cart will carry the OMSS and the electronics that must be kept in proximity to the OMSS. The OMSS will normally be mounted to the top of the cart, but will also be able to operate on a test console cabled to the cart.

Test Console. The single-rack test console presently contains most of the receiver electronics. The receiver interface panel has been fabricated for the test console. This panel contains test points and meters for monitoring the modified AGC system that has been installed in the AIL receiver. This panel also acts as the interface for data output and serves as interconnection panel between the receiver and the tracking subsystem.

High Voltage Amplifier. During installation of the components into the test console it was discovered that the +500 volt amplifier for driving the IMCs was providing a variable output of 350 to 600 volts. The amplifier was returned to the Hughes Malibu facility for repair. A +500 volt amplifier power supply was found to have failed. Rather than attempt repair, the unit was replaced with a laboratory power supply that should prove more reliable.

Stark Cell. The earlier lifetime problems with the Stark stabilization reference cells appear to be solved. The failure was traced to leaks in the high voltage connectors. Several cells using an indium washer sealing technique have now operated over a period of nearly 2 months without changing their characteristics. It is expected that these cells will have a minimum lifetime of 1 year.

Stark Cell Electronics. The final version of the control electronics has been received from the Hughes Research Laboratories. This has not yet been tested with the local oscillator laser. The remaining tasks to be completed before this test is run include fabrication and installation of the bolometer detector mount, fabrication of the interconnecting cable, and completion of laser starting tests.

Cryostat Tests. During the reporting period the cryostat was successfully tested on the test cart. The cooldown time was longer than expected, requiring about 35 minutes plus 20 minutes purge time. The bottle pressure drop during this period was from 1850 to 1500 psi while the minimum temperature reached was 84°K. It appears that gas consumption is such to require a bottle of N₂ for each day of operation.

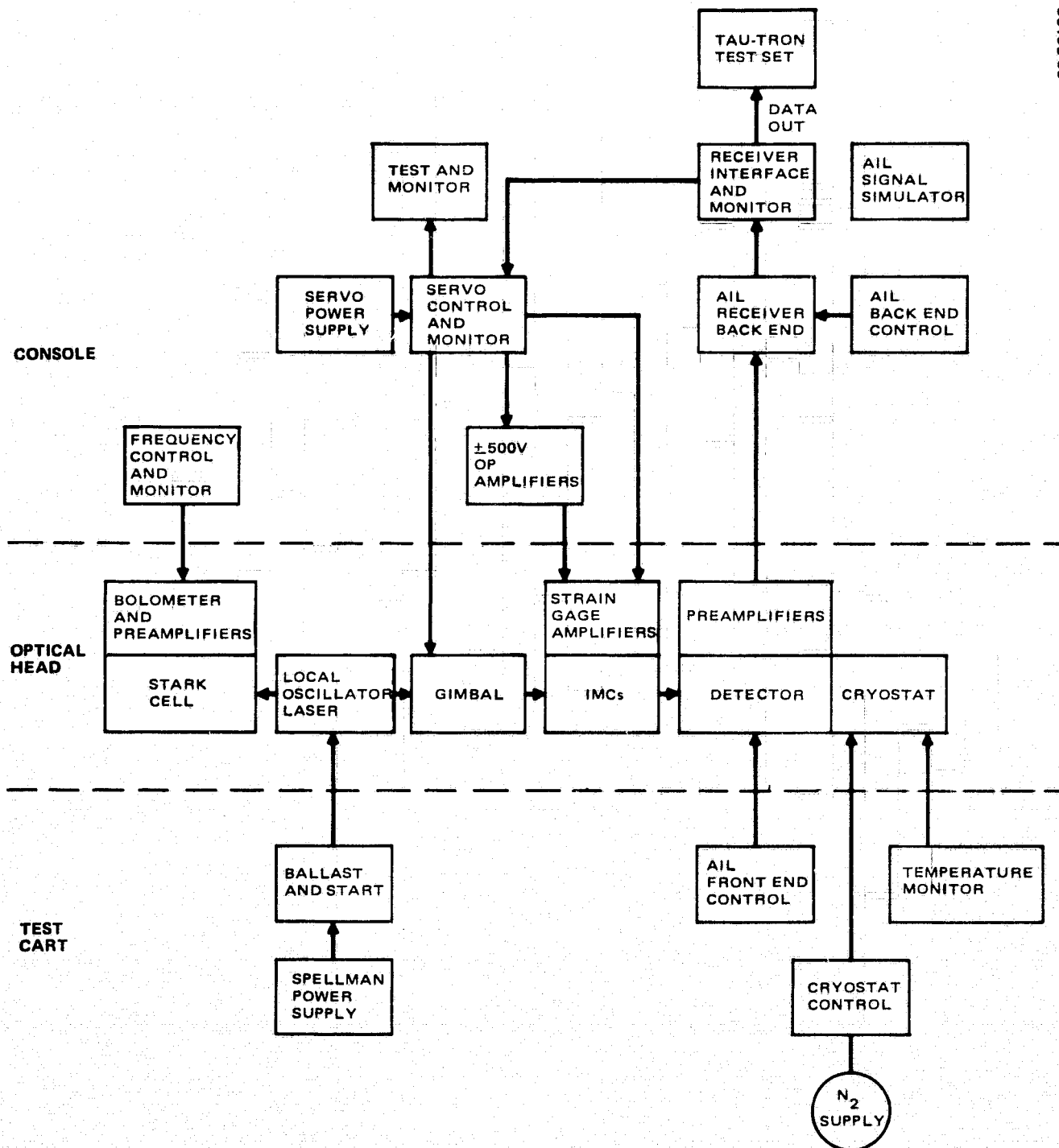
Laser Power Supply and Starting Circuit. The laser power supply was returned by Spellman after it was repaired. It is presently operating satisfactorily. The power

supply was also successfully tested with the high voltage pulsed laser starting circuit. One final test must be made to complete this subassembly, a test of the high voltage cabling. The original plan was to use high voltage coaxial cable (15 kV). However, experience with other waveguide lasers has shown that the high capacitance of such cable interacts with the power supply regulator and the laser tube resulting in an unstable discharge. To prevent this, it is necessary to use a lower capacity unshielded cabling and a separate ground return. The OMSS is presently being modified to accept unshielded wire, and it is hoped that the original coaxial connectors can still be used. Tests will be made early in the next reporting period to confirm the acceptability of these connectors. If these tests are unsatisfactory, a modification of the beryllium structure will be required.

Plans for Next Period. Due to the delay in receipt of the local oscillator subassembly (including the Stark cell, electronics, and laser power supply), the personnel scheduled for integration were diverted to other programs. Delays in these other programs prevented the return of these people to the integration task immediately upon receipt of the delayed components. However, all personnel have now been released from other programs and are working full time on the integration task.

During the next period, priority will be given to completion of testing of the local oscillator subassembly. This will include power cabling, laser starting tests, stabilization tests, and optical interface determinations. It is expected that by the end of May the local oscillator should be ready for final installation in the OMSS.

A parallel effort is being conducted to provide a Hughes test laser for the receiver. A Hughes laser is being modified to incorporate Stark stabilization into a well damped optical modulator. Although this laser/modulator combination will be optimized to operate in an optical FM format, it will be possible to use it as a coupling modulator at reduced efficiency. Full BER testing of the receiver system will not occur until the NASA transmitter breadboard is complete.



RECEIVER SYSTEM BLOCK DIAGRAM